



# Nonlinear consolidation analysis of multilayered soil with coupled vertical-radial drainage using the spectral method

Bin-Hua Xu<sup>1</sup> · Buddhima Indraratna<sup>2</sup> · Cholachat Rujikiatkamjorn<sup>2</sup> · Thanh T. Nguyen<sup>2</sup> · Ning He<sup>1,3</sup>

Received: 13 December 2021 / Accepted: 9 August 2022 / Published online: 28 October 2022  
© The Author(s) 2022

## Abstract

The nonlinear variation of soil compressibility and permeability with void ratio (i.e.,  $e$ -log  $\sigma'$  and  $e$ -log  $k$ ) has been included in the consolidation theory to accurately predict the behavior of soft soil stabilized by vertical drains. However, most current nonlinear consolidation models incorporating the coupled radial-vertical flow are based on some simplified assumptions, while including some features such as the complex implementation of multilayered computations, time-dependent loading and stress distribution with depth. This study hence introduces a novel approach where the spectral method is used to analyze the nonlinear consolidation behavior of multilayered soil associated with coupled vertical-radial drainage. In addition, time- and depth-dependent stress and soil properties at each soil layer are incorporated into the proposed model. Subsequently, the solution is verified against experimental and field data with comparison to previous analytical solutions. The results show greater accuracy of the proposed method in predicting in-situ soil behavior. A parametric study based on the proposed solution indicates that the ratio between the compression and permeability indices ( $\omega = C_c/C_k$ ) has a great impact on the consolidation rate, i.e., the greater the  $\omega$ , the smaller the consolidation rate. Increasing the load increment ratio and the absolute difference between unity and  $\omega$  (i.e.,  $|\omega - 1|$ ) can exacerbate prediction error if the conventional simplified methods are used.

**Keywords** Multilayered soil · Nonlinear consolidation · Spectral method · Vertical-radial drainage · Vertical drains

## 1 Introduction

The use of vertical drains (i.e., prefabricated vertical drains PVDs) combined with preloading to accelerate the consolidation process of soft soils is one of the most common soil improvement methods around the world [8, 11, 25, 77]. In this method, the drainage path is substantially shortened through the radial drainage induced by the drains so that the dissipation of excess pore water pressure (EPWP) becomes much faster. The radial consolidation theories were developed extensively in the past decades, resulting in various models capturing different aspects of loading, drain and soil behaviors over time and space. The following sections provides a critical review into the novelty of various theories while highlighting their limitations.

Figure 1 features most significant theoretical studies on radial consolidation. The most original close-form solution for ideal vertical drains was originally proposed by Barron [3]. Richart [55] compared the two assumptions of free

---

✉ Buddhima Indraratna  
Buddhima.Indraratna@uts.edu.au

Bin-Hua Xu  
xubinhua0416@gmail.com; bhxu@nhri.cn

Cholachat Rujikiatkamjorn  
Cholachat.Rujikiatkamjorn@uts.edu.au

Thanh T. Nguyen  
Thanh.Nguyen-4@uts.edu.au

Ning He  
nhe@nhri.cn

<sup>1</sup> Geotechnical Engineering Department, Nanjing Hydraulic Research Institute, Nanjing, China  
<sup>2</sup> Transport Research Centre, University of Technology Sydney, Ultimo, Sydney, Australia  
<sup>3</sup> Key Laboratory of Reservoir and Dam Safety, Ministry of Water Resources, Nanjing, China

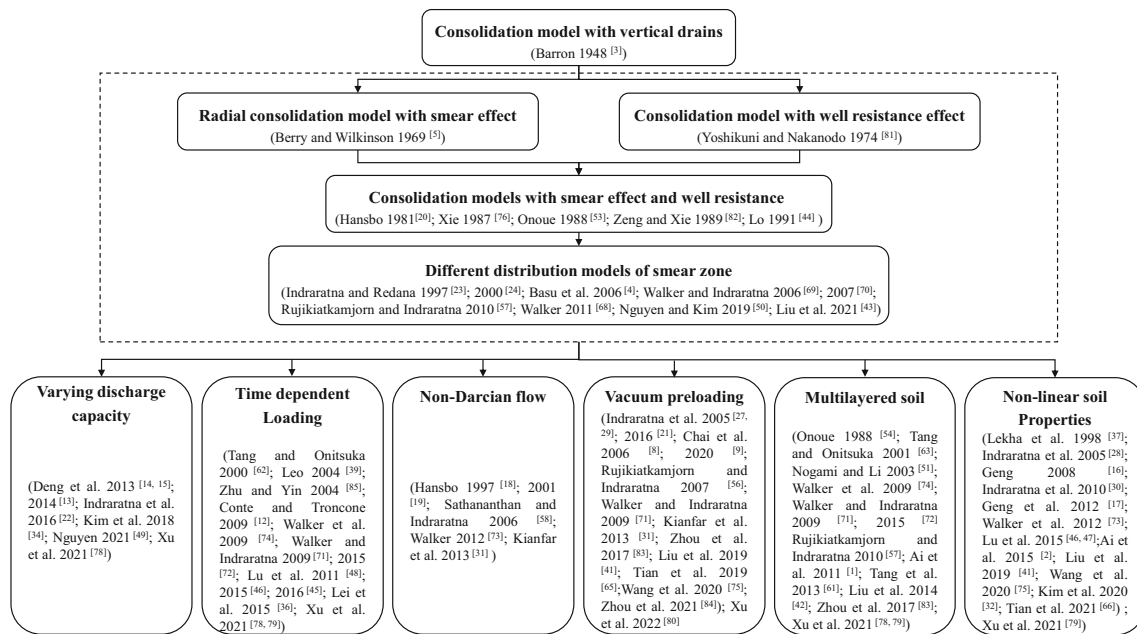


**Fig. 1** Development of consolidation models with vertical drain

strain and equal strain proposed by Barron [3] and found that the results obtained by the above two assumptions are almost the same. Berry and Wilkinson [5] and Yoshikuni and Nakanodo [81] incorporated the smear and well resistance effects for the first time. Afterward, Hansbo [20] proposed a solution that can combine both the effects of smear zone and well resistance based on the assumption of equal strain. Since then, numerous attempts were made to improve the consolidation models especially addressing the smear and well resistance effects [44, 53, 76, 82]. The salient features of those models can be highlighted as follows:

- (i) Characterization of smear zone [4, 23, 24, 43, 50, 57, 68–70];
- (ii) Time- and depth-dependent discharge capacity [13–15, 22, 34, 49, 78];
- (iii) Time-dependent preloading [12, 36, 39, 45, 46, 48, 62, 71, 72, 78, 79, 85];
- (iv) Non-Darcian flow [18, 19, 31, 58, 73];
- (v) Vacuum preloading [8, 9, 21, 27, 29, 31, 41, 56, 65, 71, 75, 80, 83, 84]; and
- (vi) Multilayered condition [1, 42, 51, 54, 57, 61, 63, 71, 72, 74, 78, 83].

Note that the above features can be combined to provide improved predictions. However, most of them were based on simplified assumptions of constant soil compressibility and permeability during consolidation.

It is well understood that when the stress range (difference between initial and final effective stress) becomes large, both soil compressibility and permeability vary with the void ratio during the consolidation process [59, 64], especially in soft clays. Some radial consolidation models considering these nonlinear variations were proposed. For example, Lekha et al. [37] and Indraratna et al. [28] obtained an analytical solution for the nonlinear radial consolidation by simplifying the differential equation. Walker et al. [73] proposed an analytical solution that can combine the non-Darcian flow with both nonlinear compressibility and permeability. Using the similar approach, Lu et al. [46] and Kim et al. [32] derived the solutions under time-dependent loading. Tian et al. [66] obtained an analytical solution based on elliptical cylindrical equivalent model. It is noteworthy that these nonlinear models can only consider radial drainage while ignoring the vertical flow when the length of vertical drains is relatively large compared to drain spacing. In shallow soft soil under railways where short vertical drains are used (e.g., PVDs with 8 m length and 2.5 m spacing were used in Sandgate railway, NSW reported by Indraratna et al. [26]), the coupled vertical-horizontal drainage analysis is pertinent as the vertical drainage can contribute significantly to the overall consolidation. While the method proposed by Carrillo [7] (i.e., Approach 1 in Fig. 2) can be adopted, this approach is only applicable when soil compressibility and permeability are constant. Although recent efforts overcame this limitation [2, 16, 17, 30, 41, 47, 75], some

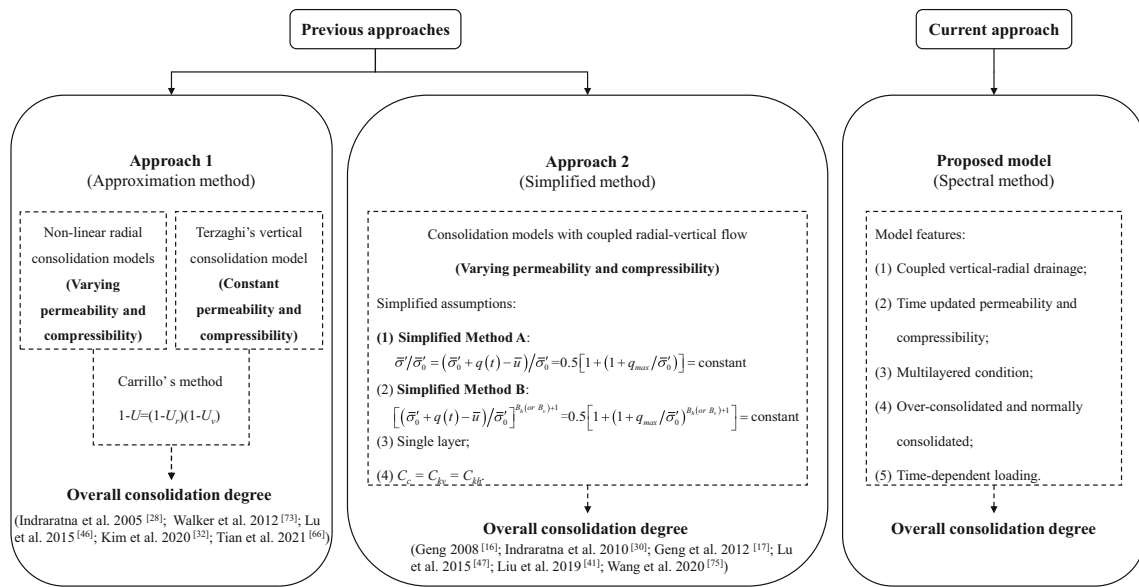


Fig. 2 Key differences in the past and current approaches for the nonlinear consolidation analysis with vertical drains

approximations or simplifications were required (e.g., single soil layer,  $C_c = C_k$  as shown in Approach 2 in Fig. 2).

As the sedimentary history and stress conditions of soil can vary significantly in the field, most soft soils are rarely homogeneous and usually consist of several layers [2]. However, previous nonlinear consolidation models show limited capacity in capturing the influence of adjacent soil layers because they strictly rely on specific loading and stress distribution patterns. This study, therefore, aims to overcome the above limitations in previous studies [71, 72, 74, 78] by considering the nonlinear compressibility and permeability based on the spectral method framework, so that a more realistic and rigorous solution for the PVD-assisted soil consolidation can be achieved. In this paper, the spectral method is adopted to solve the governing equations, and subsequently, the model is verified against the experimental and field data in comparison with previous simplified solutions. Finally, the applicability and threshold limits of the past and the current solutions are discussed and evaluated.

## 2 Limitations of existing models

This section firstly details the limitations of existing mathematical solutions, followed by the objectives and innovations of the current study. The logarithmic models ( $e'$ -log  $\sigma$  and  $e'$ -log  $k$ ) are commonly used to represent the variations of soil compressibility and permeability with void ratio, which can be represented by [64]:

$$e = \begin{cases} e_0 - C_r \log\left(\frac{\bar{\sigma}'}{\bar{\sigma}'_0}\right) & \text{for } \bar{\sigma}' \leq \bar{\sigma}'_p \\ e_0 - C_r \log\left(\frac{\bar{\sigma}'_p}{\bar{\sigma}'_0}\right) - C_c \log\left(\frac{\bar{\sigma}'}{\bar{\sigma}'_p}\right) & \text{for } \bar{\sigma}'_p < \bar{\sigma}' \end{cases} \quad (1)$$

$$e = e_0 + C_{kh} \log\left(\frac{k_h}{k_{h0}}\right) \quad (2)$$

$$e = e_0 + C_{kv} \log\left(\frac{k_v}{k_{v0}}\right) \quad (3)$$

where  $e$  is the void ratio while the subscript 0 denotes the initial state;  $C_c$ ,  $C_r$ ,  $C_{kh}$ ,  $C_{kv}$  are the compression index, the recompression index, the radial permeability index and the vertical permeability index, respectively;  $\bar{\sigma}'_0$ ,  $\bar{\sigma}'_p$  and  $\bar{\sigma}'$  are the initial effective stress, the yield stress (effective pre-consolidation pressure) and the average effective stress, respectively;  $k_h$  and  $k_v$  are the radial and vertical permeability coefficients of the undisturbed soil, respectively.

From Eqs. (1)–(3), the following relationships between effective stress and permeability and compressibility are obtained:

$$\frac{k_h}{k_{h0}} = \begin{cases} \left(\frac{\bar{\sigma}'}{\bar{\sigma}'_0}\right)^{-\frac{C_r}{C_{kh}}} & \text{for } \bar{\sigma}' \leq \bar{\sigma}'_p \\ \left(\frac{\bar{\sigma}'_p}{\bar{\sigma}'_0}\right)^{\frac{C_c - C_r}{C_{kh}}} \left(\frac{\bar{\sigma}'}{\bar{\sigma}'_p}\right)^{-\frac{C_c}{C_{kh}}} & \text{for } \bar{\sigma}'_p < \bar{\sigma}' \end{cases} \quad (4)$$

$$k_v/k_{v0} = \begin{cases} \left(\frac{\sigma'}{\sigma'_0}\right)^{-\frac{C_r}{C_{kv}}} & \text{for } \sigma' \leq \sigma'_p \\ \left(\frac{\sigma'_p}{\sigma'_0}\right)^{\frac{C_c-C_r}{C_{kv}}} \left(\frac{\sigma'}{\sigma'_0}\right)^{-\frac{C_c}{C_{kv}}} & \text{for } \sigma'_p < \sigma' \end{cases} \quad (5)$$

$$m_v = -\frac{1}{(1+e_0)} \frac{\partial e}{\partial \sigma'} = \begin{cases} \frac{C_r}{\sigma'_0(1+e_0) \ln 10} \frac{\sigma'_0}{\sigma'} & \text{for } \sigma' \leq \sigma'_p \\ \frac{C_c}{\sigma'_0(1+e_0) \ln 10} \frac{\sigma'_0}{\sigma'} & \text{for } \sigma'_p < \sigma' \end{cases} \quad (6)$$

The following parameters are now introduced and defined as:

$$A_h = 1; B_h = -\frac{C_r}{C_{kh}}; A_v = 1; B_v = -\frac{C_r}{C_{kv}}; m_{v0} = \frac{C_r}{\sigma'_0(1+e_0) \ln 10} \quad \text{for } \sigma' \leq \sigma'_p$$

$$A_h = \left(\frac{\sigma'_p}{\sigma'_0}\right)^{\frac{C_c-C_r}{C_{kh}}}; B_h = -\frac{C_c}{C_{kh}}; A_v = \left(\frac{\sigma'_p}{\sigma'_0}\right)^{\frac{C_c-C_r}{C_{kv}}}; B_v = -\frac{C_c}{C_{kv}}; m_{v0} = \frac{C_c}{\sigma'_0(1+e_0) \ln 10} \quad \text{for } \sigma'_p < \sigma'$$

Then the radial and vertical consolidation coefficients can be expressed as:

$$C_h = \frac{k_h}{\gamma_w m_v} = A_h \frac{k_{h0}}{\gamma_w m_{v0}} \left(\frac{\sigma'}{\sigma'_0}\right)^{B_h+1} \quad (7)$$

$$C_v = \frac{k_v}{\gamma_w m_v} = A_v \frac{k_{v0}}{\gamma_w m_{v0}} \left(\frac{\sigma'}{\sigma'_0}\right)^{B_v+1} \quad (8)$$

The above expressions (i.e., Eqs. (4)–(8)) show how the compression and permeability of soil would change due to the reduced void ratio during consolidation. Due to the complexity in solving the consolidation governing equations, some studies [16, 17, 30] assumed that  $B = B = -1$  based on the field situation, where the compression  $C_c$  is very close to the permeability indices ( $C_{kv}$  or  $C_{kh}$ ), while the others (summarized in Table 1) have obtained simplified analytical solutions based on the following assumptions:

- (1) Simplified Method A: use an average value to represent the ratio of the effective stress to the initial effective stress (i.e.,  $\sigma'/\sigma'_0$  in Eqs. (7) and (8)) during the consolidation process, i.e.,  $\sigma'/\sigma'_0 = (\sigma'_0 + q(t) - \bar{u})/\sigma'_0 = 0.5 [1 + (1 + q_{\max}/\sigma'_0)]$ , where  $q(t)$ ,  $q_{\max}$  and  $\bar{u}$  are the time-dependent loading, the final level of loading and EPWP, respectively [46, 47, 75];
- (2) Simplified Method B: use the average values to represent the varying consolidation coefficients, which are the nonlinear coefficient terms in the governing equation, i.e.,  $s = [(\sigma'_0 + q(t) - \bar{u})/\sigma'_0]^{B_h(or B_v)+1} =$

$$0.5 [1 + (1 + q_{\max}/\sigma'_0)^{B_h(or B_v)+1}] \quad [28, 32, 33, 35, 38, 41, 79].$$

Table 1 lists the capabilities and assumptions of some significant nonlinear consolidation models. It can be seen from Table 1 that the main limitations of previous nonlinear consolidation models are as follows:

- (a) Although Simplified Methods A and B based on Assumptions (1) and (2) adopt the void-ratio-stress relationship (Eq. (1)) for settlement and EPWP calculations, these two assumptions make the consolidation coefficients (i.e., the coefficient terms of the con-

solidation governing equation) constant. This means the nonlinear behavior is not included in the dissipation equation of EPWP properly [28, 32, 33, 35, 38, 41, 46, 47, 75].

**Table 1** Summary of previous nonlinear consolidation models

Models	Factor included			Assumptions	
	Drainage	Loading	Layer	(1)	(2)
Lekha et al. [38]	Vertical	Instantaneous	Single	No	Yes
Kim et al. [35]	Vertical	Time-dependent	Single	No	Yes
Kim et al. [33]	Vertical	Time-dependent	Multiple	No	Yes
Indraratna et al. [28]	Radial	Instantaneous	Multiple	No	Yes
Walker et al. [73]	Radial	Step-instantaneous	Multiple	No	No
Lu et al. [46]	Radial	Time-dependent	Multiple	Yes	No
Kim et al. [32]	Radial	Time-dependent	Multiple	No	Yes
Lu et al. [47]	Radial-vertical	Time-dependent	Single	Yes	No
Wang et al. [75]	Radial-vertical	Time-dependent	Single	Yes	No
Liu et al. [41]	Radial-vertical	Time-dependent	Single	No	Yes
Proposed model	Radial-vertical	Time-dependent	Multiple	No	No

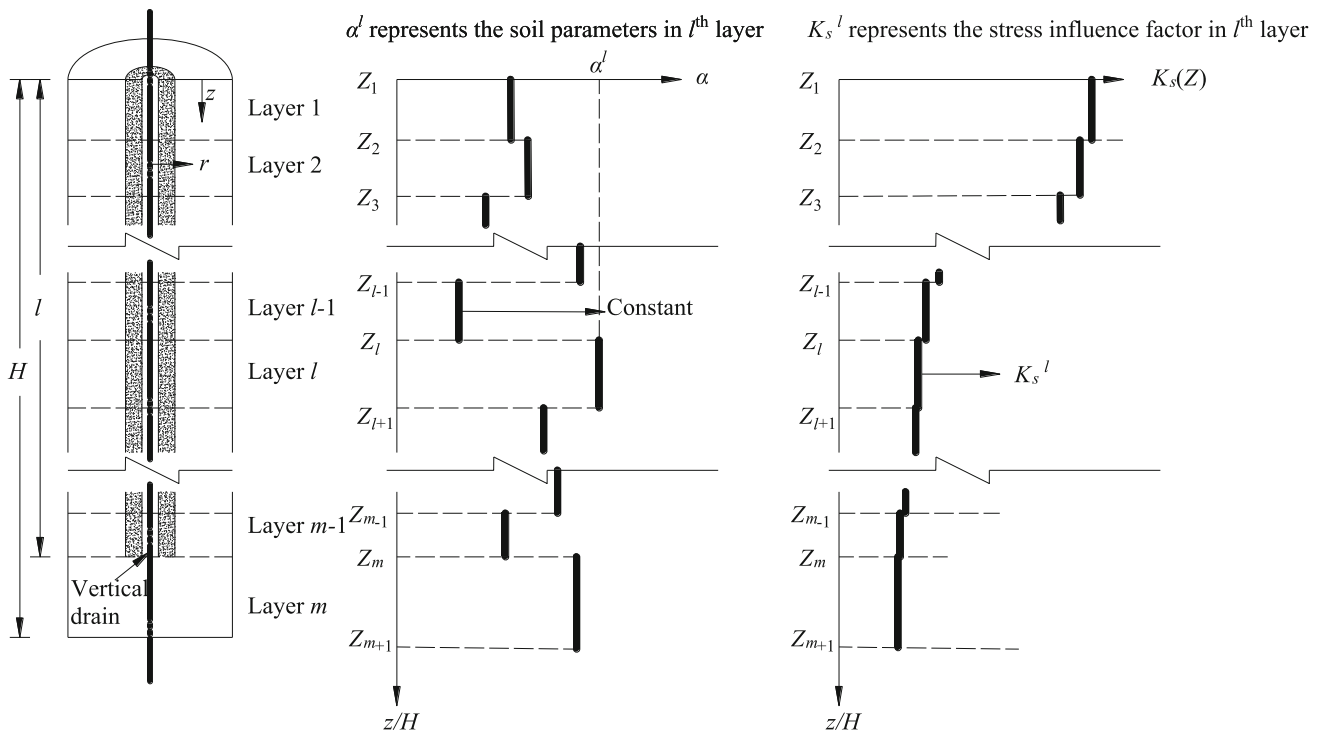


Fig. 3 Soil properties and stress distribution of multilayered soil

- (b) Simplified Methods A and B directly adopt these assumptions to linearize the nonlinear coefficient terms of the governing equation. The validity and associated threshold have not been established. In other words, the acceptance range of error caused by the simplified assumptions has not been evaluated. It is necessary to evaluate the errors induced by simplified assumptions that help understand the validity of Simplified Methods A and B, and thus determine the appropriate range of soil parameters [28, 32, 33, 35, 38, 41, 46, 47, 75].
- (c) Although some of the nonlinear consolidation models can consider coupled radial-vertical drainage, they can only consider a single layer of soil while changes in soil parameters and stress distribution along the depth are neglected [41, 47, 75].

In view of the above, the objectives of this study are to provide a more general nonlinear consolidation model which can consider the following factors:

- i. Coupled vertical-radial drainage;
- ii. Nonlinear permeability and compressibility during consolidation process;
- iii. Multilayered condition;
- iv. Time-dependent loading;

- v. Over-consolidated and normally consolidated state.

The key advantages of the current approaches are shown in Fig. 2 in comparison with conventional methods.

### 3 Theoretical Formulation

#### 3.1 Basic assumptions

The following basic assumptions in this study were adopted while developing the mathematic model.

- (a) The soil particles and water are incompressible. The nonlinear relationships between void ratio with permeability and effective stress during consolidation are shown in Eqs. (2) and (3).
- (b) The compressibility and the vertical permeability coefficients in the smear and undisturbed zones are assumed to be the same. The horizontal permeability coefficient in the smear zone is constant distribution and the ratio of horizontal permeability coefficients outside and in the smear zone is constant during consolidation. The size of the smear zone is constant throughout the depth.
- (c) The initial effective stress, the pre-consolidation pressure, the vertical stress, and associated parameters for a given *l*th layer of soil with relatively small

thickness are assumed to be constant, but they change with depth as shown in Fig. 3.

- (d) The soil is assumed to be fully saturated, and the velocity of pore water flow is governed by Darcy’s law. Although the EPWP varies in the radial direction, the average EPWP along the radial direction is used at a given depth to combined with flow in the vertical direction as shown in Eq. (9), following the approach proposed by Tang and Onitsuka [62].
- (e) Strains only occur in the vertical direction, which are equal at a given depth along the radial direction (equal strain condition).

### 3.2 Governing differential equations

The unit cell for a multilayered soil with a vertical drain is shown in Fig. 3. The governing differential equation for soil consolidation, while considering vertical and radial drainage, can be given by (see “Appendix A1” for derivation):

$$\frac{2k_{h0}A_h}{\gamma_w r_e^2 \mu} \left(\frac{\sigma'}{\sigma'_0}\right)^{B_h} \bar{u} - \frac{k_{v0}A_v}{\gamma_w H^2} \left(\frac{\sigma'}{\sigma'_0}\right)^{B_v} \frac{\partial^2 \bar{u}}{\partial Z^2} = m_{v0} \frac{\sigma'_0}{\sigma'} \frac{\partial \sigma'}{\partial t} \tag{9}$$

where  $\bar{u}$  is the average EPWP at a particular depth;  $t$  is the time;  $H$  is the total depth of soil;  $Z$  is the normalized depth, i.e.,  $Z=z/H$  in which  $z$  is the depth;  $\gamma_w$  is the unit weight of water;  $m_{v0}$  is the initial volume compressibility, and it can be calculated by

$$m_{v0} = C_c / [\sigma'_0(1 + e_0) \ln 10]$$

when  $\sigma'_p < \sigma'$  or

$$m_{v0} = C_r / [\sigma'_0(1 + e_0) \ln 10]$$

when  $\sigma' \leq \sigma'_p$ ;  $\mu$  is the dimensionless parameter, which is computed based on the permeability variation of soil within the smear zone, the radial geometry of the drain. Detailed calculation of  $\mu$  can be referred to the previous studies, e.g., Walker and Indraratna [71], Lu et al.[47] and Nguyen [49].

Given a time-dependent loading  $q(t)$ , the effective stress can be determined by:

$$\sigma' = \sigma'_0 + q(t) - \bar{u} \tag{10}$$

By defining  $C_{h0} = k_{h0}/\gamma_w m_{v0}$ ,  $C_{v0} = k_{v0}/\gamma_w m_{v0}$ ,  $dT_{h0} = 2C_{h0}/r_e^2 \mu$ ,  $dT_{v0} = C_{v0}/H^2$ , the governing equation can be rewritten as:

$$\begin{aligned} dT_{h0}A_h \left(1 + \frac{q(t) - \bar{u}}{\sigma'_0}\right)^{B_h+1} \bar{u} \\ = dT_{v0}A_v \left(1 + \frac{q(t) - \bar{u}}{\sigma'_0}\right)^{B_v+1} \frac{\partial^2 \bar{u}}{\partial Z^2} + \left(\frac{\partial q(t)}{\partial t} - \frac{\partial \bar{u}}{\partial t}\right) \end{aligned} \tag{11}$$

It can be seen from Eq. (11) that when vertical drainage is not considered and  $q(t)$  becomes the instantaneous loading, the above equation turns into the nonlinear radial consolidation model of Walker et al. [73] without considering non-Darcian flow. If the above nonlinear term is further replaced by the average value (i.e.,  $[(\sigma'_0 + q(t) - \bar{u})/\sigma'_0]^{B_h+1} = 0.5[1 + (1 + q_{max}/\sigma'_0)^{B_h+1}]$ ), it becomes the nonlinear radial consolidation model by Indraratna et al. [28]. Furthermore, when  $B_{hv} = 1$  (the slopes of  $e$ -log  $\sigma'$  and  $e$ -log  $k$  are the same, the above governing equation becomes the same as that by Hansbo [20].

### 3.3 Advanced features of spectral method

Spectral method is one of the very advanced mathematical techniques for facilitating numerical solution of even complex partial differential equations (PDEs). It evolved after the common numerical category of finite element method (FEM) and finite difference method (FDM) whose the accuracy depends on the size of the subdomain.[67]. The spectral method is based on global basis functions (high-order polynomial or trigonometric functions). Compared with the numerical methods such as FDM and FEM, the spectral method has the following advantages when the geometry of the problem is fairly smooth and regular (e.g., consolidation) [6, 52]: (1) high calculation accuracy; (2) memory-minimizing and computational efficiency; and (3) high stability. Therefore, the method can capture the transition of variables over time and space such as stress, EPWP and soil properties. It was adopted in the current study to solve the complex governing equation incorporating the variation of multiple soil properties during consolidation. When the pore pressure profile changes sharply, oscillations may occur near steep fronts, which is called the Gibbs phenomenon. The Gibbs phenomenon can be reduced or eliminated by increasing the series of  $N$  term. Therefore, more series terms are required when modeling sharp changes in the pore pressure profile.

### 3.4 Solutions based on the spectral method

For the spectral method, the EPWP  $\bar{u}(Z, t)$  is expressed as a truncated series of  $N$  terms, which can be expressed in matrix form as follows [71, 72, 74, 78]:

$$\bar{u}(Z, t) \approx \sum_{j=1}^N \Phi_j(Z)A_j(t) = \Phi A \tag{12}$$

where  $\Phi_j$  are known basis functions and  $A_j$  are expansion coefficients which can vary with time, and

$$\Phi = [\Phi_1 \quad \Phi_2 \quad \dots \quad \Phi_N] \tag{13}$$

$$A^T = [A_1 \quad A_2 \quad \dots \quad A_N] \tag{14}$$



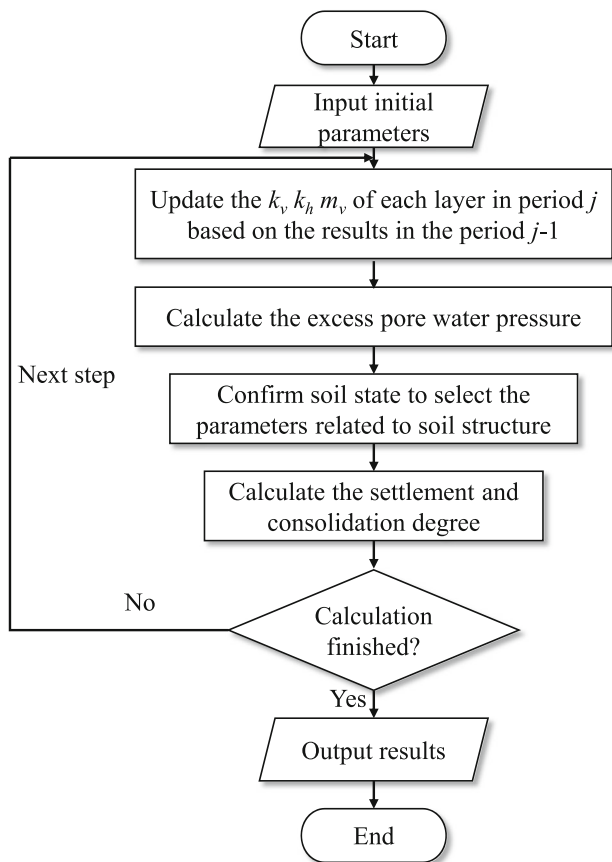


Fig. 4 Flow chart of the computational procedure for the proposed method

The choice of the basis functions needs to satisfy the boundary conditions of governing equation [6]. The pervious top-pervious bottom (PTPB) and the pervious top-impervious bottom (PTIB) boundary conditions are given, respectively, by:

$$\bar{u}(0, t) = 0 \text{ and } \bar{u}(H, t) = 0 \tag{15}$$

$$\bar{u}(0, t) = 0 \text{ and } \partial \bar{u}(H, t) / \partial Z = 0 \tag{16}$$

With respect to these boundary conditions (Eqs. (15) and (16)), the appropriate choice of basis function can be given by:

$$\Phi_j(Z) = \sin(M_j Z) \tag{17}$$

where  $M_j$

$$M_j = \begin{cases} j\pi & \text{for PTPB} \\ \pi(2j - 1)/2 & \text{for PTIB} \end{cases} \tag{18}$$

Note that in the current study, the material properties such as permeability and compressibility vary with void ratio and the effective stress, resulting in the complexity to obtain an exact solution through the spectral method. Therefore, the current study proposes a numerical approach where the consolidation process is divided into a discrete number of time steps (Fig. 4). During each time step, the material parameters are assumed to be constant, but they are then re-computed and updated in the next time step based on Eqs. (6)–(8). By updating the material properties at each time step and combining the weighted residual method (WRM),  $A(t)$  can be obtained using Eq. (19), thereby the EPWP at a given depth and time can be obtained in a matrix form (see “Appendix A2” for derivation):

$$A(t) = e^{-\int_0^t \Gamma^{-1} \Psi d\tau} \left( \int_0^t e^{\int_{-\infty}^{\tau} \Gamma^{-1} \Psi dt} \Gamma^{-1} I d\tau \right) \tag{19}$$

$$\bar{u}(Z, t) = \Phi e^{-\int_0^t \Gamma^{-1} \Psi d\tau} \int_0^t e^{\int_{-\infty}^{\tau} \Gamma^{-1} \Psi dt} \Gamma^{-1} I d\tau \tag{20}$$

where the elements of matrices  $\Gamma$ ,  $I$  and  $\Psi$  incorporate the loading patterns and material parameters of every soil layer. The detailed expressions of these elements can be found in “Appendix A2”, Eqs. (40)–(43). Figure 4 is the flowchart showing the detailed implementation of the proposed model. Note that the interval of time step affects the accuracy of the updated soil parameters for the next time step.

Since the EPWP at a given depth is expressed as a function of depth and time as shown in Eq. (20), the average pore water pressure  $\bar{u}_{\text{avg}}(Z_l, Z_{l+1}, t)$  and settlement  $S(Z_l, Z_{l+1}, t)$  in the  $l$ th layer (between depths  $Z_l$  and  $Z_{l+1}$ ) can be calculated, respectively, by:

$$\bar{u}_{\text{avg}}(Z_l, Z_{l+1}, t) = \frac{\int_{Z_l}^{Z_{l+1}} \Phi dZ}{Z_{l+1} - Z_l} A(t) \tag{21}$$

$$S(Z_l, Z_{l+1}, t) = \begin{cases} \frac{C_r^l H}{1 + \bar{e}_0^l} \int_{Z_l}^{Z_{l+1}} \log\left(\frac{\bar{\sigma}^l}{\bar{\sigma}_0^l}\right) dZ & \text{for } \bar{\sigma}^l \leq \bar{\sigma}_p^l \\ \frac{C_r^l H}{1 + \bar{e}_0^l} \int_{Z_l}^{Z_{l+1}} \log\left(\frac{\bar{\sigma}_p^l}{\bar{\sigma}_0^l}\right) dZ + \frac{C_c^l H}{1 + \bar{e}_0^l} \int_{Z_l}^{Z_{l+1}} \log\left(\frac{\bar{\sigma}^l}{\bar{\sigma}_p^l}\right) dZ & \text{for } \bar{\sigma}^l < \bar{\sigma}^l \end{cases} \tag{22}$$

The overall average degrees of consolidation for the multilayered soil defined by the excess pore pressure and settlement can, respectively, be obtained by:

$$U_p = \frac{\sum_{l=1}^m [q(t)K_s^l - \bar{u}_{avg}(Z_l, Z_{l+1}, t)]}{\sum_{l=1}^m [q_{max}K_s^l]} \tag{23}$$

$$U_s = \frac{\sum_{l=1}^m S(Z_l, Z_{l+1}, t)}{\sum_{l=1}^m S(Z_l, Z_{l+1}, \infty)} \tag{24}$$

where  $Z_l$  and  $Z_{l+1}$  denote the normalized depth at the bottom and top of the  $l$ th layer, respectively;  $K_s^l$  is the stress influence factor in the  $l$ th layer;  $S(Z_l, Z_{l+1}, \infty)$  is the final settlement in the  $l$ th layer. The superscript  $l$  represents the value of the corresponding parameter or variable at the  $l$ th layer.

### 3.5 Continuity conditions at the soil interface

In the solution of the spectral method, the average EPWP  $\bar{u}(Z, t)$  is expressed as a truncated series of  $N$  terms, and the sine functions were selected as the basis functions. Therefore, the value of the average EPWP and its derivative in the soil at any position are continuous.

First, the continuous condition of EPWP at the interface between two adjacent layers ( $l$ th and  $l + 1$ th layer) can be satisfied:

$$\bar{u}(l)|_{Z_l} = \bar{u}(l + 1)|_{Z_l} \tag{25}$$

In addition, since the soil property of a certain soil layer is assumed to be constant in this study, an interface (i.e., dummy) layer with a thickness of zero is set between two adjacent layers, as shown in Fig. 3. The soil parameters are assumed to be linearly distributed in the interface layer, so the continuous condition of flow rate can also be satisfied between two adjacent layers ( $l$ th and  $l + 1$ th layer), i.e.,

$$k_v^l \frac{\partial \bar{u}(l)}{\partial Z} \Big|_{Z=Z_l} = k_v^{l+1} \frac{\partial \bar{u}(l + 1)}{\partial Z} \Big|_{Z=Z_l} \tag{26}$$

It is noteworthy that the distribution made by the dummy layer to  $\Gamma_{ij}$  and  $I_i$  is zero, and the distribution made by the interface layer between two adjacent layers ( $l^{th}$  and  $l + 1^{th}$  layer) to  $\Psi_{ij}$  can be found in Eq. 43.

## 4 Model verification

To verify this proposed model, the mathematical formulation presented above is applied to the following laboratory and field studies:

1. Radial consolidation of single soil layer by single-instantaneous loading [28, 73];
2. Vertical and radial consolidation of multilayered soil by multi-ramp loading [10, 60];

The calculation of the dimensionless drain parameter  $\mu$  is based on the assumption of a smear zone with constant reduced permeability [20].

### 4.1 Laboratory tests

Two laboratory studies [28, 73] were used to verify the proposed model. The physical size of the consolidation apparatus was 450 mm in diameter by 950 mm high, and the reconstituted alluvial clay from Moruya (New South Wales) was used. For these tests (normal consolidation range), the initial pre-consolidation pressures  $\bar{\sigma}'_0$  of the soil were 20 kPa and 50 kPa with the loading increments in these two studies were 30 kPa and 50 kPa, respectively (i.e.,  $\Delta p = 30, 50$  kPa). The detailed testing procedure can be found in Walker et al. [73]. The soil parameters and drain properties are shown in Table 2. Note that as the drain was relatively short, the well resistance effect was neglected in the calculation of  $\mu$ .

The degree of consolidation based on the settlement is obtained using Eq. (24). The accuracy of the calculation is determined by the selection of the truncated series  $N$ , as shown in Eq. (12). An investigation on the convergence was carried out especially addressing the effects of the numbers of the truncated series  $N$  through these two

**Table 2** Soil parameters and drain properties of the model test (after Walker et al. [73])

Parameters	Test 1	Test 2
$C_c$	0.29	0.29
$C_{kh}$	0.45	0.45
Diameter of influence zone, $D_e$ (m)	0.45	0.45
Diameter of equivalent drain, $D_w$ (m)	0.066	0.066
Diameter of smear zone, $D_s$ (m)	0.2	0.2
Initial horizontal permeability $k_{h0}$ ( $10^{-10}$ m/s)	4.4	4.0
$k_f/k_s$	1.5	1.5
Initial void ratio, $e_0$	1.000	0.950
Initial height, $H$ /m	0.925	0.870
Pre-consolidation pressure, $\bar{\sigma}'_0$ ( $\bar{\sigma}'_p$ )/kPa	20	50
Load, $p$ /kPa	30	50



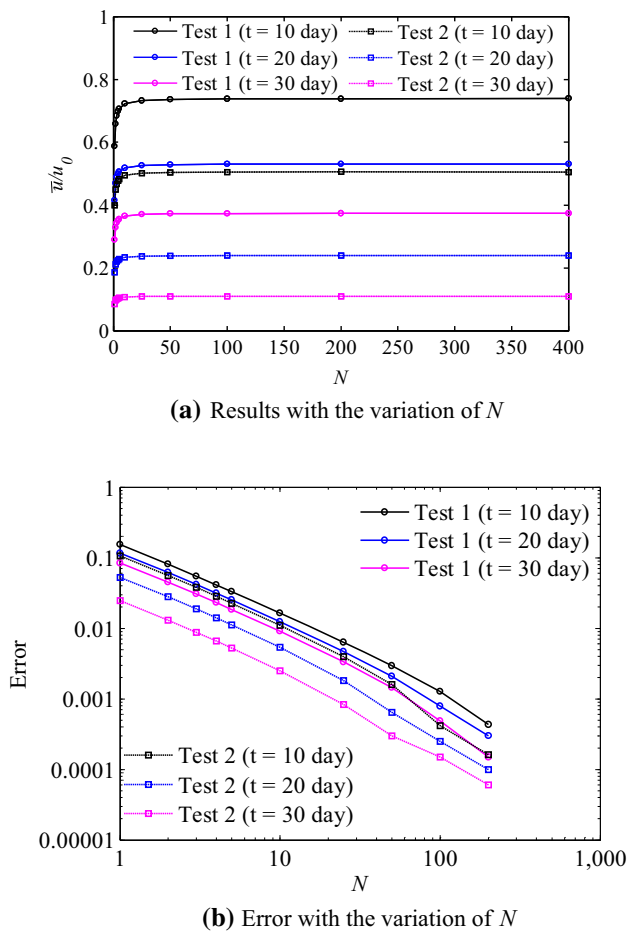


**Fig. 5** Investigation on the solution convergence over the truncated series  $N$

laboratory tests, the results are shown in Fig. 5. It shows that  $N = 50$  are sufficient for a single soil layer with an error  $< 0.5\%$  for calculating EPWP. In addition, Fig. 5b shows the “exponential” convergence of spectral method with  $N$ . The relationship between  $N$  and error  $\delta$  can be expressed as  $\log(N) = a + b \log(\delta)$ , where  $a$  and  $b$  are the coefficients. In practical applications, the selection of  $N$  depends on the complexity of the problem (e.g., the number of soil layers and the differences in parameters between soil layers) and the required accuracy of computation. When the number of soil layers is large or the soil parameters differ greatly, the value of  $N$  should be larger to improve the calculation accuracy and eliminate the influence of the Gibbs phenomenon [6, 52]. The appropriate truncation series  $N$  can be selected according to the calculation accuracy requirements. For example, if the number of digit accuracy ( $p$ ) is required, the truncated series  $N$  can be selected based on the relationship of  $N = 10^{a+b \log(10^{-p})}$  in this case. In these two tests, only radial drainage was allowed, so  $dT_{r,0}$  was set as 0. The results were compared with the laboratory data and the analytical

solutions presented by Indraratna et al. [28], Walker et al. [73] and Lu et al. [46], as shown in Fig. 6a. Note that the model of Walker et al. [73] is a closed-form analytical solution, while the models of Lu et al. [46] and Indraratna et al. [28] are simplified analytical solutions based on Simplified Methods A and B, respectively. Figure 6 shows that the results calculated by the proposed method are very close to the experimental results and analytical solution of Walker et al. [73]. Indeed, Fig. 6b and c shows that the largest deviations between the proposed solution and measured data and analytical solutions [73] in Test 1 and Test 2 are less than 4.6% and 0.6%, respectively. The difference between the calculation results of the proposed method and the analytical solution of Walker et al. [73] is caused by the insufficient value of truncation series  $N$ . When the value of  $N$  increases, the result predicted by the proposed method becomes more accurate and closer to the analytical solution. However, the results from the models of Lu et al. [46] and Indraratna et al. [28] deviate from accuracy, especially in the early stage of consolidation. This is because the average consolidation coefficients have been in these two models, which overestimate the actual consolidation coefficient during the early stage, as shown in Fig. 6d and e.

## 4.2 Hangzhou–Ningbo (HN) Expressway, China

The test embankment using PVDs at Hangzhou–Ningbo (HN) Expressway was reported by Chai et al. [10] and Shen et al. [60]. The HN Expressway was located at the southern coast of Hangzhou Bay, China. The thickness of the soft layers was about 23 m. The top crust was considered to be in lightly over-consolidated state with an over-consolidation ratio (OCR) of about 5, and the deeper layers were in the normally consolidated state. The soil profile and soil parameters used in this study provided by Chai et al. [10] are shown in Table 3. The stage loading process is shown in Fig. 7a. The final fill height for the surcharge preloading was 5.88 m and the unit weight of the fill material was  $20 \text{ kN/m}^3$ . As suggested by Tavenas et al. [64], the permeability indices in this study were calculated by  $C_{kh} = C_{hv} = 0.5e_0$ . Parameters related to the vertical drain are as follows: (a) the geometrical parameters  $d_e = 1.580 \text{ m}$ ,  $d_s = 0.355 \text{ m}$ ,  $d_w = 0.053 \text{ m}$ ,  $n = r_e/r_w = 29.8$ ,  $s = r_s/r_w = 6.7$ , and  $l = 19.0 \text{ m}$ ; (b) the permeability ratio  $(k_h/k_s) = 13.8$ ; and (c) the discharge capacity ( $q_w$ )  $100 \text{ m}^3/\text{year}$ .

The surface settlement and EPWPs were calculated using Eqs. (19)–(22) with 100 series terms ( $N$ ) and the results are shown in Figs. 7b and 8 in comparison with the measured data and the predictions using previous models [32, 46, 74]. Note that the model of Walker et al. [74] is the conventional linear consolidation model for multilayered

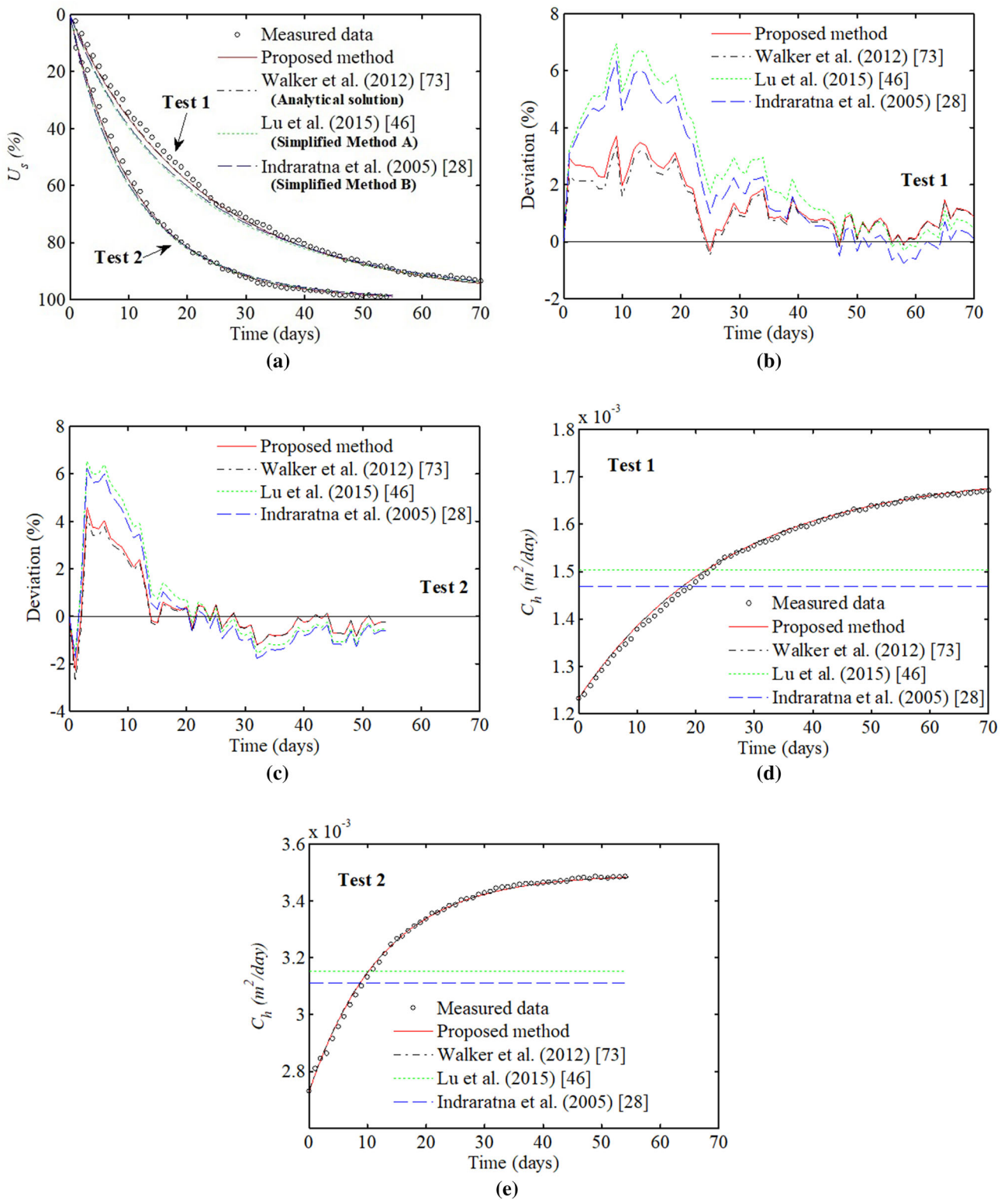


**Fig. 6** Comparison between the proposed model and those by Indraratna et al. [28], Walker et al. [73] and Lu et al. [46]; **a** consolidation degree; **b** deviation in Test 1; **c** deviation in Test 2; **d** horizontal consolidation coefficient variation in Test 1; **e** horizontal consolidation coefficient variation in Test 2

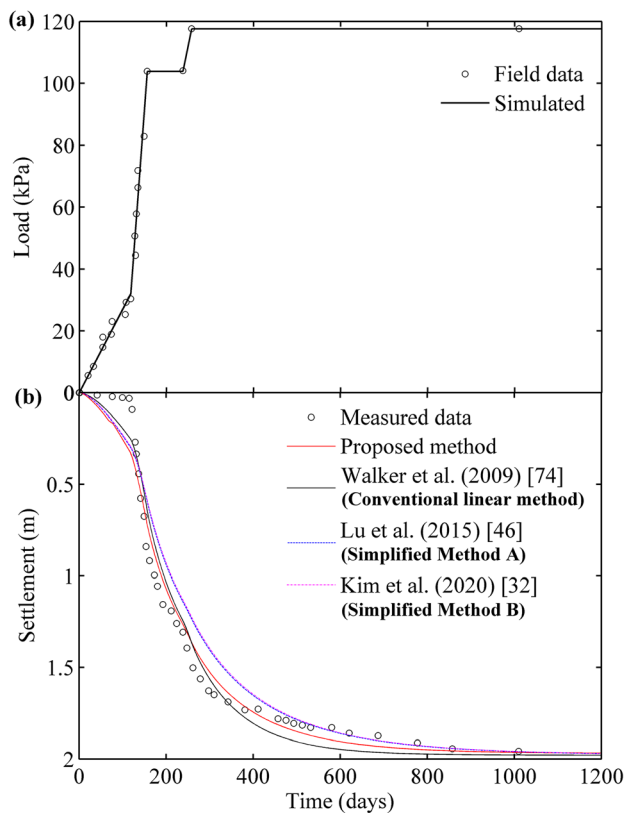
**Table 3** Soil parameters for subsoil in the test embankment at Hangzhou–Ningbo Expressway, China (modified after Chai et al. [10])

Depth (m)	$\gamma$ (kN/m <sup>3</sup> )	$m_v$ ( $10^{-3}$ kPa <sup>-1</sup> )	$e_0$	$C_c$	$C_r$	$k_{v0}$ ( $10^{-3}$ m/d)	$k_{h0}$ ( $10^{-3}$ m/d)	$\bar{\sigma}'_0$ at middle of layer (kPa)	OCR
0.0–1.0	19.3	0.68	0.81	0.184	0.018	3.03	3.03	4.65	5.0
1.0–3.0	18.5	0.68	1.07	0.370	0.037	1.00	2.00	17.80	1.1
3.0–4.8	18.5	1.28	1.07	0.370	0.037	0.22	0.56	33.95	1.1
4.8–6.8	17.3	0.93	1.36	0.690	0.069	0.30	0.80	48.90	1
6.8–8.3	17.3	1.32	1.36	0.690	0.069	0.30	0.80	61.68	1
8.3–10.3	17.3	1.15	1.36	0.650	0.065	0.30	0.80	74.45	1
10.3–12.3	17.3	0.96	1.36	0.650	0.065	0.28	0.52	89.05	1
12.3–14.3	17.3	0.86	1.36	0.650	0.065	0.28	0.52	103.65	1
14.3–16.3	17.9	0.77	1.10	0.458	0.046	0.16	0.35	118.85	1
16.3–18.3	17.9	0.55	1.10	0.458	0.046	0.16	0.35	134.65	1
18.3–19.0	19.3	0.51	0.81	0.230	0.023	0.04	0.06	145.81	1

soil with coupled vertical-radial drainage, the initial permeability coefficients ( $k_{h0}$  and  $k_{v0}$ ) and compressibility coefficient ( $m_v$ ) were adopted in the linear consolidation model, as shown in Table 3. The settlements predicted by the model of Walker et al. [74] overestimate the field data due to the inability to consider the nonlinear behavior of the soil. The models of Lu et al. [46] and Kim et al. [32] are analytical solutions of radial consolidation (i.e., only radial drainage) based on the Simplified Methods A and B,

respectively, which can be considered as the piecewise solutions in which the soil parameters and stress conditions are the corresponding values at the mid-point of each layer. Since the ratios between the compression and permeability indices of the main compression soil layer (e.g., 4.8–19 m) are close to 1 in this case (see Table 3), the settlements predicted by the models of Lu et al. [46] and Kim et al. [32] are very similar. However, since the nonlinear vertical permeability are not included in these two models, their predicted settlements underestimate the field data. The proposed method which incorporates both nonlinear vertical and radial permeability provides better prediction. For example, the difference between the predicted and measured settlement at 400 days significantly decreases to about 10 mm (0.58%) using the proposed model, where the errors in the analyses of Walker et al. [74], Lu et al. [46] and Kim et al. [32] are 71 mm (4.11%), 82 mm (4.73%) and 87 mm (5.02%), respectively.

Figure 8 compares the predicted EPWPs by the current proposed solution with the measured data and the results obtained by the methods of Walker et al. [74], Lu et al. [46] and Kim et al. [32] at three different depths (i.e.,  $z = -2.0$  m,  $z = -10.0$  m and  $z = -14.05$  m). The EPWPs predicted by the model of Walker et al. [74] overestimate the dissipation rate of EPWPs at all depths, as this model cannot consider the nonlinear behaviors of the soil. Generally, the results by the proposed method are closer to the field data compared to other models, especially in shallow soil, i.e., at depth of 2 m. For example, at 200 days, the error of 30 kPa in previous models is reduced to be less than 3 kPa by the proposed model. At greater depths (i.e.,  $z = -10.0$  m and  $z = -14.05$  m), the ratios between the compression and permeability indices ( $C_c/C_{kh}$  and  $C_c/C_{kv}$ ) are close to 1, and the soil consolidation is predominantly governed by the radial drainage. Therefore, the EPWPs predicted by models of Lu et al. [46] and Kim et al. [32] approach closer to the field data and the current

**Fig. 7** Comparison of settlement curves: **a** loading process; **b** surface settlement comparison

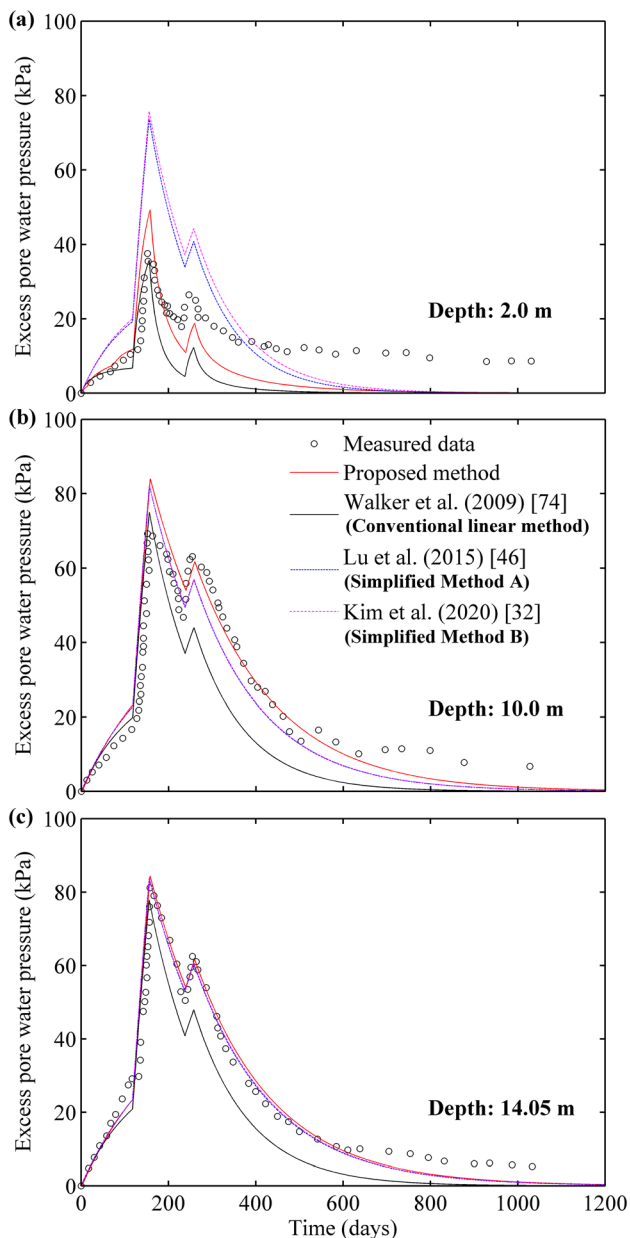


**Fig. 8** Comparison of predicted EPWPs of test embankment with the field data: **a** at depth  $z = -2.0$  m; **b** at depth  $z = -10.0$  m; **c** at depth  $z = -14.05$  m

model, as shown in Fig. 8b and c. Note that all the predicted EPWPs dissipate completely after 800 days while the measured EPWPs gradually change after 600 days. For example, the measured EPWP at 2 m depth remains almost unchanged at about 10 kPa until the end of observation. This residual EPWP could be attributed to the effect of rising groundwater level after 600 days.

Figure 9 shows the distribution of EPWP along the depth at 100, 200 and 400 days. In general, the isochrones of EPWP are in good agreement with the measured data. In fact, the predicted curves present very well the smooth

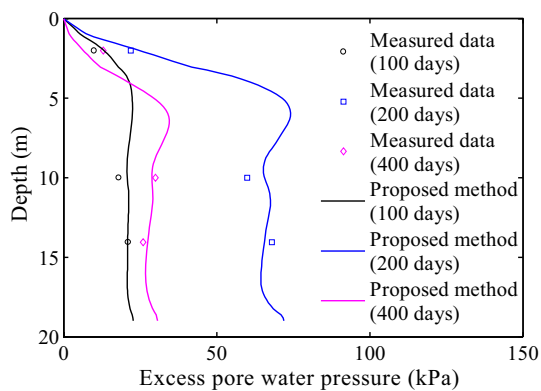


**Fig. 9** The isochrones of excess pore water pressure at  $t = 100, 200$  and  $400$  days obtained by the proposed method

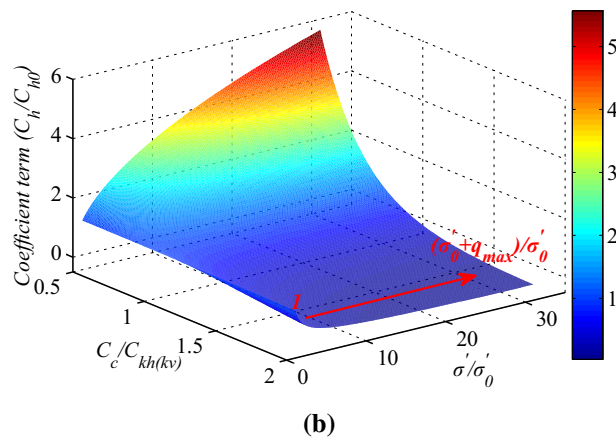
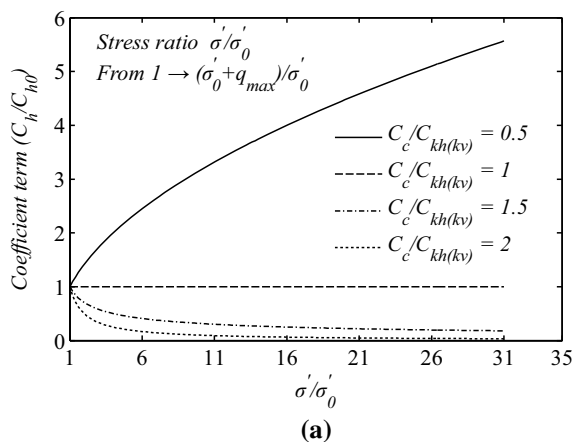


**Fig. 10** Variation of nonlinear coefficient term: **a** coefficient term vary with stress ratio in consolidation process; **b** variation of nonlinear terms with the stress ratio and  $C_c/C_{kh(or kv)}$

transition in EPWP over different soil layers, provided appropriate value of  $N$ . This shows that the proposed model based on the spectral method can be well applied to the nonlinear consolidation calculation of multilayered foundations.

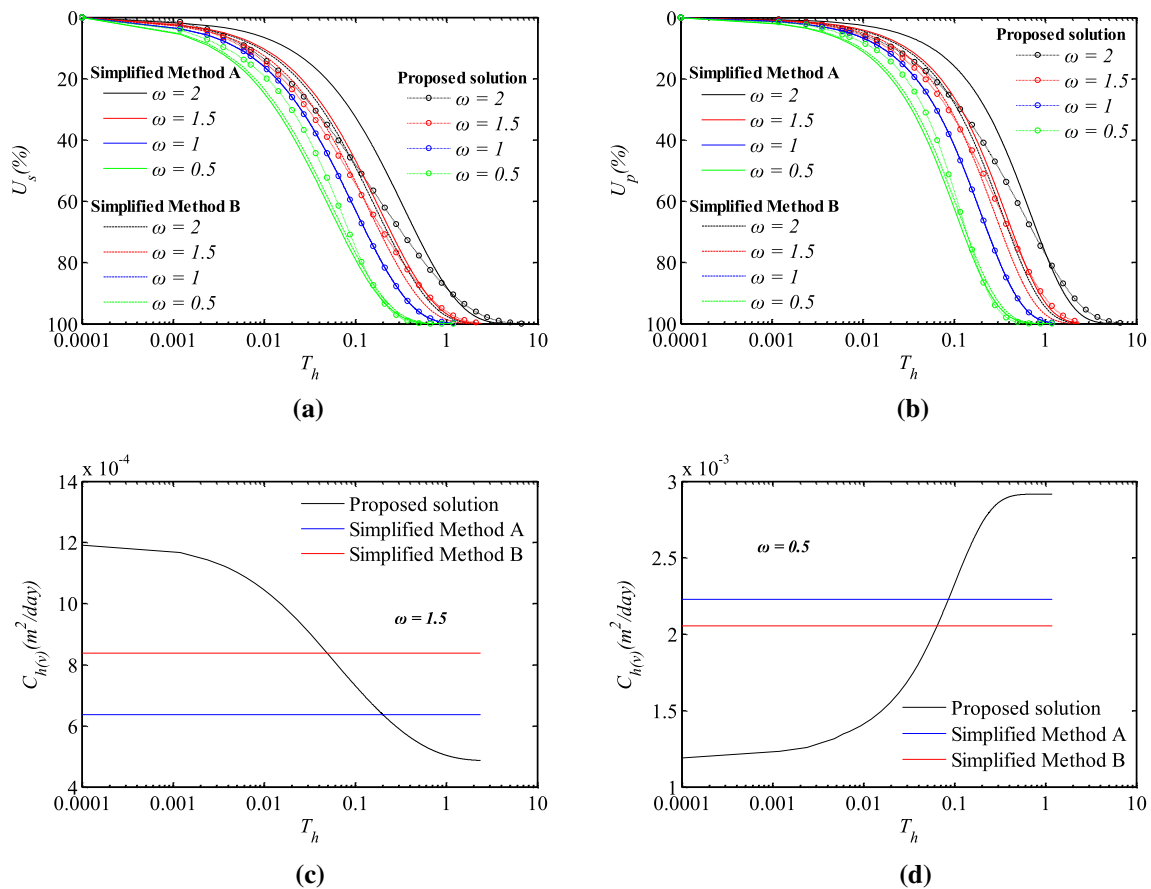


**Fig. 11** Comparison between the proposed solution and simplified solutions for different  $\omega$ : **a** average degree of consolidation ( $U_s$ ) based on settlement; **b** average degree of consolidation ( $U_p$ ) based on EPWP; **c** comparison of consolidation coefficient variation ( $\omega = 1.5$ ); **d** comparison of consolidation coefficient variation ( $\omega = 0.5$ )

The above verifications prove that the current consolidation model based on spectral method can improve the prediction significantly especially at shallow layers where the vertical drainage can contribute considerably to the overall soil consolidation. The proposed solution is suitable for analyzing vertical and radial consolidation to capture more realistic conditions such as multilayered soils and time-dependent loading associated with nonlinear behaviors of compressibility and permeability.

### 5 Assessment of past and current nonlinear consolidation solutions

As discussed earlier, the simplified analytical solutions for nonlinear consolidation can be obtained based on certain assumptions for simplicity. While for previous models based on Assumption (1) (i.e., assuming that  $(\bar{\sigma}'/\bar{\sigma}'_0)^{B_h(or B_v)+1} = \{0.5[1 + (1 + q_{max}/\bar{\sigma}'_0)]\}^{B_h(or B_v)+1}$ ) and Assumption (2) (i.e., assuming that  $(\bar{\sigma}'/\bar{\sigma}'_0)^{B_h(or B_v)+1} = 0.5[1 + (1 + q_{max}/\bar{\sigma}'_0)^{B_h(or B_v)+1}]$ ), the limitation of these

two assumptions has not been investigated. Indeed, the values of the nonlinear coefficient terms  $(\bar{\sigma}'/\bar{\sigma}'_0)^{B_h(or B_v)+1}$  are mainly determined by the ratios  $B_h$  (or  $B_v$ ) (i.e.,  $-C_c/C_{kh}$  or  $-C_c/C_{kv}$ ) and  $\bar{\sigma}'/\bar{\sigma}'_0$ . It can be seen from Fig. 10a that when the compression index ( $C_c$ ) is not equal to the permeability indexes ( $C_{kv}$  or  $C_{kh}$ ), the nonlinear coefficient term changes significantly during the consolidation process (i.e.,  $\bar{\sigma}'/\bar{\sigma}'_0$  changes from 1 to  $(\bar{\sigma}'_0 + q_{max})/\bar{\sigma}'_0$ ). Moreover, Fig. 10b indicates that the nonlinear coefficient term changes more apparently with the increase in the effective stress ratio when  $C_c/C_{kh(or kv)}$  is less than 1. For example, the coefficient term increases sharply toward 5 when  $C_c/C_{kh(or kv)} = 0.5$  and  $(\bar{\sigma}'_0 + q_{max})/\bar{\sigma}'_0 = 25$ .

Therefore, in this section, the consolidation responses based on the Simplified Methods A and B have been obtained using the average value of  $(\bar{\sigma}'/\bar{\sigma}'_0)^{B_h(or B_v)+1}$  appeared in Eq. (37), and compared with those using the proposed solution. Since the main influencing factors of the nonlinear coefficient terms are  $C_c/C_{kh(or kv)}$  and  $q_{max}/\bar{\sigma}'_0$ , the effects of these two ratios are investigated through the



parametric study. The well resistance is neglected, and the imposed drainage condition is the PTIB (impervious bottom) with an instantaneous loading. The single layer normally consolidated soil ( $\bar{\sigma}'_0 = \bar{\sigma}'_p$ ) is considered isotropic ( $C_{v0} = C_{h0}$ ,  $C_k = C_{kh} = C_{kv}$ ). The soil properties based on the Moruya clay (New South Wales) were assumed as follows: (i) the soil properties:  $C_{v0} = C_{h0} = 1.2 \times 10^{-3}$  m<sup>2</sup>/day,  $\bar{\sigma}'_0 = 20$  kPa,  $C_c = 0.3$ ,  $C_k = C_{kh} = C_{kv} = 0.45$ ,  $e_0 = 1$ ; (ii) the permeability ratio ( $k_h/k_s$ ) = 1.5; and (iii) the geometrical parameters of drains:  $r_e = 0.5$  m,  $r_s = 0.222$  m,  $r_w = 0.074$  m,  $n = r_e/r_w = 6.79$ ,  $s = r_s/r_w = 3.02$ ,  $H = 5$  m,  $\mu = 1.718$ . Note that series terms in relation to  $N = 50$  were used in the analysis.

### 5.1 Effect of the ratio between the compression and permeability indices ( $C_c/C_k$ )

To study the impact of the ratio of  $C_c/C_k$  ( $\omega$ ), in the range of 0.5–2 was adopted in the analysis according to Berry and Wilkinson [5], the load increment ratio  $q_{\max}/\bar{\sigma}'_p$  was set as 5. Figure 11 (where  $T_h = C_{h0}t/d_e^2$ ) shows the comparison between the proposed and simplified solutions for different

$\omega$ . Apparently,  $\omega$  has a great impact on the consolidation rate. It shows that given the same soil parameters and load conditions, the greater the value of  $\omega$ , the smaller the consolidation rate. This is because the consolidation coefficient decreases as  $\omega$  increases, as shown in Eqs. (7) and (8). It can also be seen that when  $\omega$  is greater than 1 (black and red lines), the results of the two simplified solutions are quite different from the results by the proposed method. This is because the consolidation coefficients of Simplified Methods are greater than the varying consolidation coefficient adopted in the proposed solution in the early stage, and smaller in the later stage, as shown in Fig. 11c (take  $\omega = 1.5$  as an example). This results in the consolidation rate being lower in the early stage and larger in the later stage for both Simplified Methods. When  $\omega$  is less than 1 (green lines), an opposite trend is observed. When  $\omega$  is equal to 1 (blue line), i.e., the nonlinear terms (i.e.,  $(\bar{\sigma}'/\bar{\sigma}'_0)^{1-\omega}$ ) of all approaches are constant, all results obtained by all methods are the same, i.e., the solid, dotted and dashed blue lines coincide. In general, Simplified Method A has a larger deviation in early stage, while Simplified Method B has a larger deviation in later stage for both  $U_s$  and  $U_p$  with different values of  $\omega$ . This is

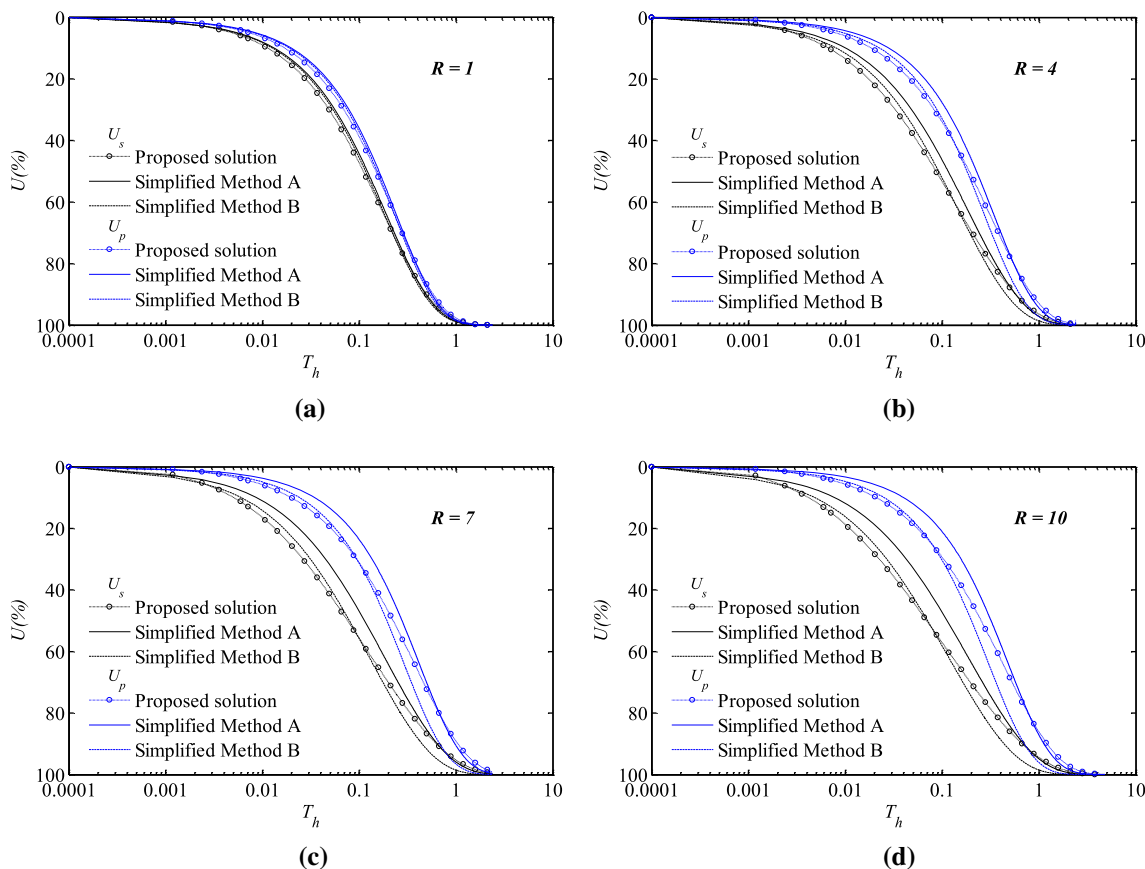


**Fig. 12** Comparison between the proposed solution and simplified solutions under different load increment ratio  $R$  for  $\omega = 1.5$ : **a**  $R = 1$ ; **b**  $R = 4$ ; **c**  $R = 7$ ; **d**  $R = 10$



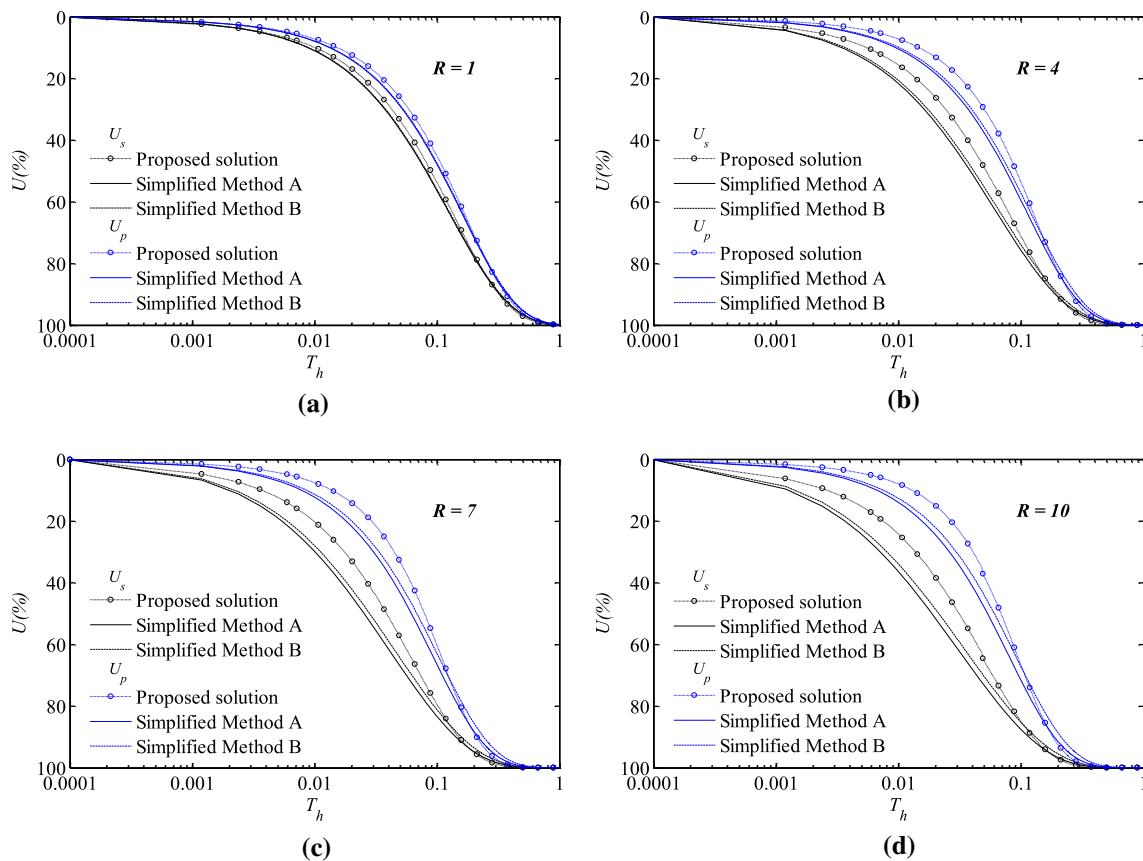


**Fig. 13** Comparison between the proposed solution and simplified solutions under different load increment ratio  $R$  for  $\omega = 0.5$ : **a**  $R = 1$ ; **b**  $R = 4$ ; **c**  $R = 7$ ; **d**  $R = 10$

caused by the magnitude of the difference between the average consolidation coefficients adopted by Simplified Methods and the variable consolidation coefficient used in the proposed method, which can be seen from Fig. 11c and d.

## 5.2 Effect of load increment ratio $q_{\max}/-\bar{\sigma}'_0$

The load increment ratio  $q_{\max}/\bar{\sigma}'_0$  ( $R$ ) is related to the applied preloading and the in-situ initial stress. The greater the load ( $q_{\max}$ ) or the smaller of in-situ initial stress ( $\bar{\sigma}'_0$ ), the greater the load increment ratio  $R$ . To study the impact of load increment ratio ( $R$ ) in the range of 1–10, four different values of  $R$  were selected under the two cases of  $\omega = 1.5$  and  $\omega = 0.5$ : (i)  $R = 1$ ; (ii)  $R = 4$ ; (iii)  $R = 7$ ; and (iv)  $R = 10$  (Figs. 12 and 13).

For  $\omega = 1.5$ , the increase in load increment ratio reduces the consolidation rate based on EPWP (i.e.,  $U_p$ ), as shown in Fig. 12. In contrast, the consolidation rate increases as  $R$  increases when  $\omega = 0.5$  (see Fig. 13). This is because the consolidation coefficient decreases as  $R$  increases when  $\omega > 1$ , and increases with the increase of  $R$  when  $\omega < 1$ , as shown in Fig. 10. It can also be seen that the results from the two simplified solutions are quite different from those

by the proposed solution. When  $R$  is small (i.e.,  $R = 1$ ), the differences in the computational results between the simplified and the proposed solutions are relatively small (the largest difference given by both simplified solutions is less than 3.5%), as shown in Figs. 12 and 13. As the load increment ratio  $R$  increases, the deviation of the simplified solutions gradually becomes significant. When  $\omega = 1.5$ , Simplified Method A has a relatively small deviation in the later stage of consolidation ( $T_h > 0.5$ ), and the Simplified Method B has a relatively small deviation in the early stage of consolidation ( $T_h < 0.1$ ). When  $\omega = 0.5$ , the results of Simplified Methods A and B are relatively close, but overall, Simplified Method B has a smaller deviation. For  $\omega = 1.5$  and  $\omega = 0.5$ , the biggest difference between the simplified solutions and proposed solution reaches 12.5% and 11.0%, respectively, when  $R = 10$ .

## 5.3 Applicability of the simplified solutions

The above analysis indicates that the simplified solutions can cause noticeable deviations in the predicted results depending on the magnitude of  $\omega$  and  $R$ . The simplified solutions must be applied in an appropriate range to maintain their prediction's accuracy. For this purpose, the

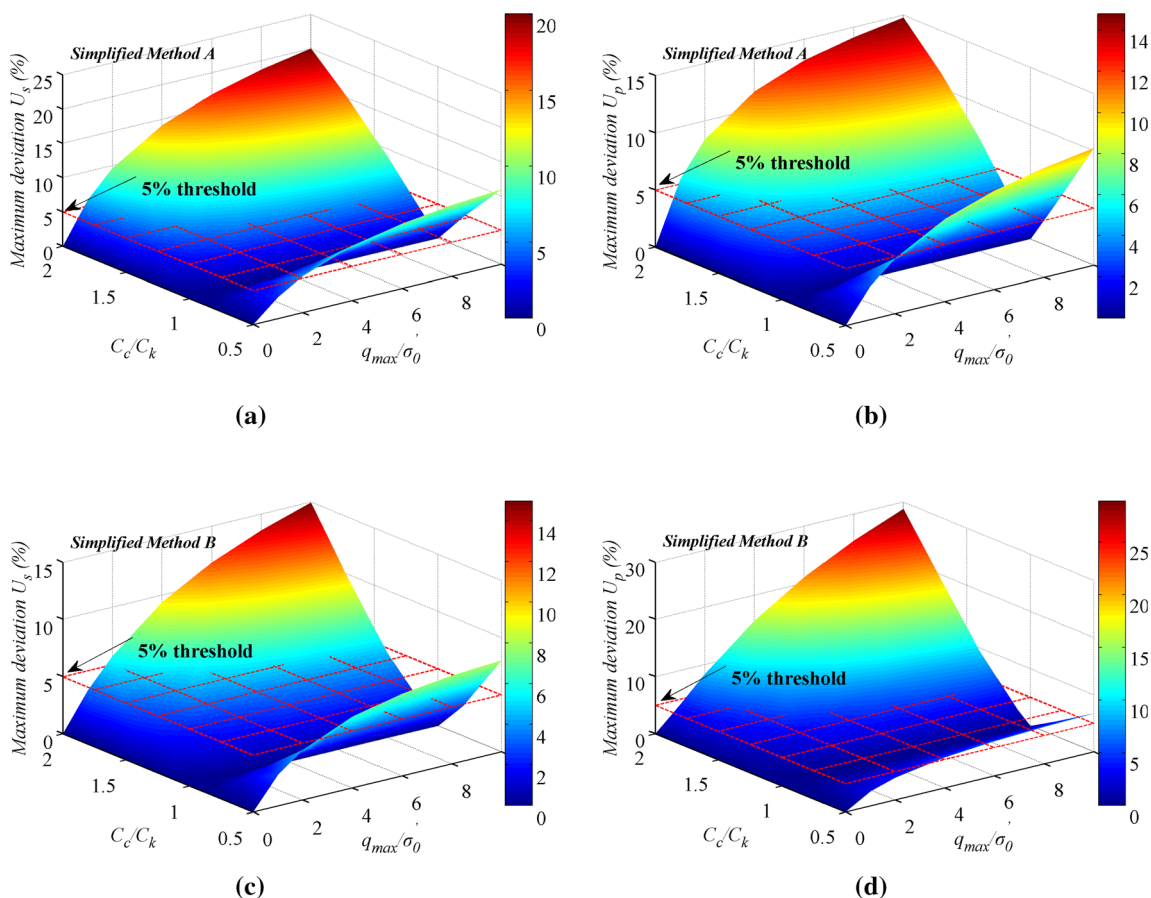


**Fig. 14** Maximum deviation in the predicted consolidation degree between the proposed solution and Simplified Methods: **a**  $U_s$  for Simplified Method A; **b**  $U_p$  for Simplified Method A; **c**  $U_s$  for Simplified Method B; **d**  $U_p$  for Simplified Method B

typical values of  $C_c/C_k$  for soil in the range of 0.5–2 were used and the range of load increment ratio  $q_{max}/\sigma'_0$  was selected within 0.1–10.

Figure 14 shows the maximum deviations in the degrees of consolidation between the proposed solution and the Simplified Methods A and B for different values of  $\omega$  and  $R$ . Obviously, the deviation of both Simplified Methods A and B increases with the increase of  $R$  and  $|\omega - 1|$ . In this study, the deviations originated by Simplified Methods A and B both reach the maximum values, i.e., 20.1% and 28.9%, respectively, when  $\omega = 2$  and  $R = 10$ . If 5% error is taken as the acceptable threshold considering the deviation in predicted results, when considering the degree of consolidation based on settlement (i.e.,  $U_s$ ), Simplified Methods A and B can only satisfy this requirement if the following conditions are met:

- (i)  $0.50 < \omega < 1.50$  when  $R < 2$ ; or  $0.75 < \omega < 1.10$  when  $2 < R < 10$  (Simplified Method A).
- (ii)  $0.50 < \omega < 1.60$  when  $R < 3$ ; or  $0.70 < \omega < 1.30$  when  $3 < R < 10$  (Simplified Method B).

When considering the degree of consolidation based on EPWP (i.e.,  $U_p$ ), Simplified Methods A and B can only satisfy the requirement if the following conditions are met:

- (i)  $0.50 < \omega < 1.60$  when  $R < 2$ ; or  $0.75 < \omega < 1.25$  when  $2 < R < 10$  (Simplified Method A).
- (ii)  $0.50 < \omega < 1.35$  when  $R < 4$ ; or  $0.65 < \omega < 1.25$  when  $4 < R < 10$  (Simplified Method B).

When the degree of consolidation based on settlement and EPWP both needs to be considered, Simplified Methods A and B can only satisfy the requirement if the combined conditions are met:

- (i)  $0.50 < \omega < 1.50$  when  $R < 2$ ; or  $0.75 < \omega < 1.10$  when  $2 < R < 10$  (Simplified Method A).
- (ii)  $0.50 < \omega < 1.35$  when  $R < 3$ ; or  $0.70 < \omega < 1.25$  when  $3 < R < 10$  (Simplified Method B).

Combining the above conditions for a general case, it can be concluded that both Simplified Methods A and B can provide acceptable predictions below 5% error when either the load increment ratio is relatively low ( $R < 2$ ) or the compression index is close to the permeability index

( $0.75 < \omega < 1.10$ ). It is noteworthy that the assumption for the smear zone would affect the value of the dimensionless parameter  $\mu$ . However, since the difference between the simplified solutions and the proposed solution is essentially the determination of nonlinear term  $\left(1 + \frac{q(t) - \bar{u}}{\bar{\sigma}_0}\right)^{B_n(\text{or } B_v)+1}$ , the value of  $\mu$  has a slight influence on the deviation from accuracy when adopting simplified solutions by additional computational verification. In this regard, the assumption for the smear zone would not change the related conclusions to any significant extent.

## 6 Model limitations

Although the proposed model can predict the nonlinear consolidation of stratified soil induced by vertical drains, it still has some limitations due to some assumptions made for facilitating the mathematical formulations and solutions. Some of these limitations are listed below:

- (a) The spectral-Galerkin method solution can lead to oscillations when the problem is represented by a discontinuous function; these oscillations are known as Gibbs phenomenon [67]. Therefore, more series terms are required when modeling sharp changes in the pore pressure profile.
- (b) The constitutive relationship associated with preloading removal has not been considered in this study.

## 7 Conclusions

In this paper, a novel approach was proposed where the spectral method was used to analyze the nonlinear consolidation of multilayered soil with coupled vertical-radial drainage. The logarithmic compressibility and permeability model ( $e$ -log  $\sigma'$  and  $e$ -log  $k$ ) was adopted to describe the nonlinear relationships. Conclusions can be drawn as follows:

- (1) The proposed method can capture well the nonlinear characteristics in consolidation behavior of different soil layers with time and depth. The application of this method to existing laboratory and field data in comparison with other analytical solutions verified the feasibility and accuracy of the proposed model. For the case study, the difference between the predicted and measured settlement at 400 days significantly decreased from 5.02% (i.e., 87 mm) by the previous models to 0.58% (10 mm) by the proposed model.

- (2) The value of  $\omega$  ( $C_c/C_k$ ) had a great impact on the consolidation rate, i.e., the greater the value of  $\omega$ , the smaller the consolidation rate. Increasing the load increment ratio ( $R = q_{\max}/\bar{\sigma}'_0$ ) and the deviation of the ratio  $\omega$  from unity (i.e.,  $|\omega - 1|$ ) can lead to a larger deviation of both Simplified Methods A and B.
- (3) Simplified Methods A and B provided accurate prediction within 5% error if the following conditions were met: (a)  $0.50 < \omega < 1.50$  when  $R < 2$ ; or  $0.75 < \omega < 1.10$  when  $2 < R < 10$  for Simplified Method A; and (b)  $0.50 < \omega < 1.35$  when  $R < 3$ ; or  $0.70 < \omega < 1.25$  when  $3 < R < 10$  for Simplified Method B.

## Appendix A: Derivation of governing equation and solutions by using the spectral method

### A.1: Derivation of governing equation

The rate of strain can be expressed as:

$$\frac{\partial \varepsilon_v}{\partial t} = -\frac{1}{(1+e_0)} \frac{\partial e}{\partial t} = m_{v0} \frac{\bar{\sigma}'_0}{\bar{\sigma}'} \frac{\partial \bar{\sigma}'}{\partial t} = \begin{cases} \frac{C_r}{\bar{\sigma}'_0(1+e_0) \ln 10} \frac{\bar{\sigma}'_0}{\bar{\sigma}'} \frac{\partial \bar{\sigma}'}{\partial t} & \text{for } \bar{\sigma}' \leq \bar{\sigma}'_p \\ \frac{C_c}{\bar{\sigma}'_0(1+e_0) \ln 10} \frac{\bar{\sigma}'_0}{\bar{\sigma}'} \frac{\partial \bar{\sigma}'}{\partial t} & \text{for } \bar{\sigma}'_p < \bar{\sigma}' \end{cases} \quad (27)$$

It is assumed that the flow rate in the unit cell is equal to the rate of change in the volume of the soil mass, then the continuity equation can be expressed by:

$$\pi(r_e^2 - r^2) \frac{\partial \varepsilon_v}{\partial t} = \pi(r_e^2 - r^2) \frac{1}{\gamma_w H^2} \frac{\partial}{\partial Z} \left( -k_v \frac{\partial \bar{u}}{\partial Z} \right) + 2\pi r \frac{k}{\gamma_w} \frac{\partial u}{\partial r} \quad (28)$$

where  $k$  is the radial permeability coefficient,  $k = k_s$  and  $k_h$  inside and outside the smear zone, respectively.

The average EPWP in the soil cylinder at depth  $Z$  is calculated from the following algebraic expression:

$$\pi(r_e^2 - r_w^2) \bar{u} = \int_{r_w}^{r_e} 2\pi r u dr \quad (29)$$

By substituting Eq. (27) into (28), the following equation expressed by the average EPWP can be obtained:

$$\bar{u} = \frac{\gamma_w r_e^2 \mu}{2k_h} \left[ \frac{1}{\gamma_w H^2} \frac{\partial}{\partial Z} \left( k_v \frac{\partial \bar{u}}{\partial Z} \right) + \frac{\partial \varepsilon_v}{\partial t} \right] \quad (30)$$

where  $\mu$  is the dimensionless parameter, which is computed based on the variation of soil permeability within the smear zone and the radial geometry of the drain.

Based on Eqs. (2)–(5), (27) and assumptions (a)–(e), the governing equation can be expressed as:

$$\frac{2k_{h0}A_h}{\gamma_w r_e^2 \mu} \left(\frac{\sigma'}{\sigma'_0}\right)^{B_h} \bar{u} - \frac{k_{v0}A_v}{\gamma_w H^2} \left(\frac{\sigma'}{\sigma'_0}\right)^{B_v} \frac{\partial^2 \bar{u}}{\partial Z^2} = m_{v0} \frac{\sigma'_0}{\sigma'} \frac{\partial \sigma'}{\partial t} \quad (31)$$

### A.2: Solutions by using the spectral method

By substituting Eq. (12) into Eq. (9) and using the spectral-Galerkin method, the governing differential equations can be rewritten as:

$$\Gamma \frac{\partial \mathbf{A}}{\partial t} + \Psi \mathbf{A} = \mathbf{I} \quad (32)$$

By using the method of variation of parameters, the solution to the non-homogeneous Eq. (30) can be found by:

$$\mathbf{A}(t) = e^{-\int_0^t \Gamma^{-1} \Psi d\tau} \left( \int_0^t e^{\int_{-\infty}^{\tau} \Gamma^{-1} \Psi dt} \Gamma^{-1} \mathbf{I} d\tau \right) \quad (33)$$

To present the explicit matrix element expressions for  $\Gamma$ ,  $\Psi$  and  $\mathbf{I}$  in a concise manner, some shorthand notations are adopted as shown below:

$$SN[\beta] = [\sin(\beta Z_{l+1}) - \sin(\beta Z_l)]/\beta \quad (34)$$

$$CS[\beta] = [\cos(\beta Z_{l+1}) - \cos(\beta Z_l)]/\beta \quad (35)$$

$$M_i = \begin{cases} i\pi & \text{for PTPB} \\ \pi(2i - 1)/2 & \text{for PTIB} \end{cases} \quad (36)$$

$$M_j = \begin{cases} j\pi & \text{for PTPB} \\ \pi(2j - 1)/2 & \text{for PTIB} \end{cases} \quad (37)$$

$$M^\pm = M_j \pm M_i \quad (38)$$

$$\Lambda_{ij}^\pm = \begin{cases} SN[M^-] \pm SN[M^+] & i \neq j \\ [Z_{l+1} - Z_l] \pm SN[M^+] & i = j \end{cases} \quad (39)$$

The contribution made by the  $l$ th layer of soil to  $\Gamma_{ij}$ ,  $\Psi_{ij}$  and  $\mathbf{I}_i$  is given by:

$$\Gamma_{ij}(l) = m_{v0}^l \frac{\sigma_0^l}{\sigma^l} \Lambda_{ij}^- \quad (40)$$

$$\Psi_{ij}(l) = \frac{2k_{h0}^l A_h^l}{\gamma_w r_e^2 \mu} \left(1 + \frac{q^l(t) - \bar{u}^l}{\sigma_0^l}\right)^{B_h} \Lambda_{ij}^- + \frac{k_{v0}^l A_v^l}{\gamma_w H^2} \left(1 + \frac{q^l(t) - \bar{u}^l}{\sigma_0^l}\right)^{B_v} M_i M_j \Lambda_{ij}^+ \quad (41)$$

$$I_i(l) = -2m_{v0}^l \frac{\sigma_0^l}{\sigma^l} \frac{\partial q^l(t)}{\partial t} CS[M_i] \quad (42)$$

Since the thickness of the interface layer is zero, the distribution made by the interface layer made by the interface layer between two adjacent layers ( $l$ th and  $l + 1$ th layer) to  $\Psi_{ij}$  is given by:

$$\Psi_{ij}(l) = -\frac{1}{\gamma_w H^2} M_j \left[ \begin{aligned} &k_{v0}^{l+1} A_v^{l+1} \left(1 + \frac{q^{l+1}(t) - \bar{u}^{l+1}}{\sigma_0^{l+1}}\right)^{B_v^{l+1}} \\ &-k_{v0}^l A_v^l \left(1 + \frac{q^l(t) - \bar{u}^l}{\sigma_0^l}\right)^{B_v^l} \end{aligned} \right] \cos(M_j Z_l) \sin(M_i Z_l) \quad (43)$$

If the number of layers is  $m$ , the final values for  $\Gamma_{ij}$ ,  $\Psi_{ij}$  and  $\mathbf{I}_i$  are given by adding the contribution of each layer of soil:

$$\Gamma_{ij} = \sum_{l=1}^m \Gamma_{ij}(l) \quad (44)$$

$$\Psi_{ij} = \sum_{l=1}^m \Psi_{ij}(l) \quad (45)$$

$$I_i = \sum_{l=1}^m I_i(l) \quad (46)$$

**Acknowledgements** This research is sponsored by the National Key Research and Development Program of China (Grant No. 2021YFC3000103), the Joint Funds of the National Natural Science Foundation of China (Grant No. U2040221) and the National Natural Science Foundation of China (Grant No. 51979174). The Authors also acknowledge the support from the Transport Research Centre, University of Technology Sydney.

**Funding** Open Access funding enabled and organized by CAUL and its Member Institutions.

**Open Access** This article is licensed under a Creative Commons Attribution 4.0 International License, which permits use, sharing, adaptation, distribution and reproduction in any medium or format, as long as you give appropriate credit to the original author(s) and the source, provide a link to the Creative Commons licence, and indicate if changes were made. The images or other third party material in this article are included in the article’s Creative Commons licence, unless indicated otherwise in a credit line to the material. If material is not included in the article’s Creative Commons licence and your intended use is not permitted by statutory regulation or exceeds the permitted use, you will need to obtain permission directly from the copyright holder. To view a copy of this licence, visit <http://creativecommons.org/licenses/by/4.0/>.

**Data availability** The data used to support the findings of this study are available from the corresponding author upon request.

### References

1. Ai ZY, Cheng YC, Zeng WZ (2011) Analytical layer-element solution to axisymmetric consolidation of multilayered soils.

- Comput Geotech 38:227–232. <https://doi.org/10.1016/j.compgeo.2010.11.011>
2. Ai ZY, Hu YD (2015) Multi-dimensional consolidation of layered poroelastic materials with anisotropic permeability and compressible fluid and solid constituents. *Acta Geotech* 10:263–273. <https://doi.org/10.1007/s11440-013-0296-6>
  3. Barron RA (1948) Consolidation of fine-grained soils by drain wells. *Trans Am Soc Civ Eng* 113:718–742. <https://doi.org/10.1061/TACEAT.0006098>
  4. Basu D, Basu P, Prezzi M (2006) Analytical solutions for consolidation aided by vertical drains. *Geomech Geoenviron* 1:63–71. <https://doi.org/10.1080/17486020500527960>
  5. Berry PL, Wilkinson WB (1969) The radial consolidation of clay soils. *Géotechnique* 19:253–284. <https://doi.org/10.1680/geot.1969.19.4.534>
  6. Boyd JP (2000) Chebyshev and Fourier spectral methods, 2nd edn. DOVER Publications Inc, New York
  7. Carrillo N (1942) Simple two and three dimensional case in the theory of consolidation of soils. *J Math Phys* 21:1–5. <https://doi.org/10.1002/sapm19422111>
  8. Chai JC, Carter JP, Hayashi S (2006) Vacuum consolidation and its combination with embankment loading. *Can Geotech J* 43:985–996. <https://doi.org/10.1139/T06-056>
  9. Chai J-C, Fu H-T, Wang J, Shen S-L (2020) Behaviour of a PVD unit cell under vacuum pressure and a new method for consolidation analysis. *Comput Geotech* 120:103415. <https://doi.org/10.1016/j.compgeo.2019.103415>
  10. Chai J-C, Shen S-L, Miura N, Bergado DT (2001) Simple method of modeling PVD-improved subsoil. *J Geotech Geoenviron Eng* 127:965–972. [https://doi.org/10.1061/\(asce\)1090-0241\(2001\)127](https://doi.org/10.1061/(asce)1090-0241(2001)127)
  11. Chu J, Yan SW, Yang H (2000) Soil improvement by the vacuum preloading method for an oil storage station. *Géotechnique* 50:625–632. <https://doi.org/10.1680/geot.2000.50.6.625>
  12. Conte E, Troncone A (2009) Radial consolidation with vertical drains and general time-dependent loading. *Can Geotech J* 46:25–36. <https://doi.org/10.1139/T08-101>
  13. Deng Y-B, Liu G-B, Lu M-M, Xie K-H (2014) Consolidation behavior of soft deposits considering the variation of prefabricated vertical drain discharge capacity. *Comput Geotech* 62:310–316. <https://doi.org/10.1016/j.compgeo.2014.08.006>
  14. Deng Y-B, Xie K-H, Lu M-M (2013) Consolidation by vertical drains when the discharge capacity varies with depth and time. *Comput Geotech* 48:1–8. <https://doi.org/10.1016/j.compgeo.2012.09.012>
  15. Deng Y-B, Xie K-H, Lu M-M et al (2013) Consolidation by prefabricated vertical drains considering the time dependent well resistance. *Geotext Geomembr* 36:20–26. <https://doi.org/10.1016/j.geotextmem.2012.10.003>
  16. Geng X (2008) Non-linear consolidation of soil with vertical and horizontal drainage under time-dependent loading. In: Proceedings of the 2008 international conference on advanced computer theory and engineering. IEEE Computer Society, Phuket, Thailand, pp 800–804
  17. Geng X, Indraratna B, Rujikiatkamjorn C, Kelly RB (2012) Non-linear analysis of soft ground consolidation at the Ballina by-pass. In: Proceedings of ‘ground engineering in a changing world’, the 11th Australia New Zealand conference on geomechanics. Australian Geomechanics Society and the New Zealand Geotechnical Society, Melbourne, Australia, pp 197–202
  18. Hansbo S (1997) Aspects of vertical drain design: Darcian or non-Darcian flow. *Géotechnique* 47:983–992. <https://doi.org/10.1680/geot.1997.47.5.983>
  19. Hansbo S (2001) Consolidation equation valid for both Darcian and non-Darcian flow. *Géotechnique* 51:51–54. <https://doi.org/10.1680/geot.2001.51.1.51>
  20. Hansbo S (1981) Consolidation of fine-grained soils by prefabricated drains. In: Proceedings of the 10th international conference on soil mechanics and foundation engineering. A A Balkema Publishers, Stockholm, Sweden, pp 677–682
  21. Indraratna B, Kan ME, Potts D et al (2016) Analytical solution and numerical simulation of vacuum consolidation by vertical drains beneath circular embankments. *Comput Geotech* 80:83–96. <https://doi.org/10.1016/j.compgeo.2016.06.008>
  22. Indraratna B, Nguyen TT, Carter J, Rujikiatkamjorn C (2016) Influence of biodegradable natural fibre drains on the radial consolidation of soft soil. *Comput Geotech* 78:171–180. <https://doi.org/10.1016/j.compgeo.2016.05.013>
  23. Indraratna B, Redana IW (1997) Plane strain modeling of smear effects associated with vertical drains. *J Geotech Eng* 123:474–478. [https://doi.org/10.1061/\(ASCE\)1090-0241\(1997\)123:5\(474\)](https://doi.org/10.1061/(ASCE)1090-0241(1997)123:5(474))
  24. Indraratna B, Redana IW (2000) Numerical modeling of vertical drains with smear and well resistance installed in soft clay. *Can Geotech J* 37:132–145. <https://doi.org/10.1139/t99-115>
  25. Indraratna B, Rujikiatkamjorn C, Ameratunga J, Boyle P (2011) Performance and prediction of vacuum combined surcharge consolidation at port of Brisbane. *J Geotech Geoenviron Eng* 137:1009–1018. [https://doi.org/10.1061/\(asce\)gt.1943-5606.0000519](https://doi.org/10.1061/(asce)gt.1943-5606.0000519)
  26. Indraratna B, Rujikiatkamjorn C, Ewers B, Adams M (2010) Class A prediction of the behavior of soft estuarine soil foundation stabilized by short vertical drains beneath a rail track. *J Geotech Geoenviron Eng* 136:686–696. [https://doi.org/10.1061/\(asce\)gt.1943-5606.0000270](https://doi.org/10.1061/(asce)gt.1943-5606.0000270)
  27. Indraratna B, Rujikiatkamjorn C, Sathananthan I (2005) Analytical and numerical solutions for a single vertical drain including the effects of vacuum preloading. *Can Geotech J* 42:994–1014. <https://doi.org/10.1139/t05-029>
  28. Indraratna B, Rujikiatkamjorn C, Sathananthan L (2005) Radial consolidation of clay using compressibility indices and varying horizontal permeability. *Can Geotech J* 42:1330–1341. <https://doi.org/10.1139/t05-052>
  29. Indraratna B, Sathananthan I, Rujikiatkamjorn C, Balasubramaniam AS (2005) Analytical and numerical modeling of soft soil stabilized by prefabricated vertical drains incorporating vacuum preloading. *Int J Geomech* 5:114–124. [https://doi.org/10.1061/\(ASCE\)1532-3641\(2005\)5:2\(114\)](https://doi.org/10.1061/(ASCE)1532-3641(2005)5:2(114))
  30. Indraratna B, Geng X, Rujikiatkamjorn C (2010) Nonlinear analysis for a single vertical drain including the effects of preloading considering the compressibility and permeability of the soil. *GeoFlorida 2010: advances in analysis. Modeling & design*. American Society of Civil Engineers, Orlando, USA, pp 147–156
  31. Kianfar K, Indraratna B, Rujikiatkamjorn C (2013) Radial consolidation model incorporating the effects of vacuum preloading and non-Darcian flow. *Géotechnique* 63:1060–1073. <https://doi.org/10.1680/geot.12.P.163>
  32. Kim P, Kim HS, Kim YG et al (2020) Nonlinear radial consolidation analysis of soft soil with vertical drains under cyclic loadings. *Shock Vib* 2020:8810973. <https://doi.org/10.1155/2020/8810973>
  33. Kim P, Kim HS, Pak CU et al (2021) Analytical solution for one-dimensional nonlinear consolidation of saturated multi-layered soil under time-dependent loading. *J Ocean Eng Sci* 6:21–29. <https://doi.org/10.1016/j.joes.2020.04.004>
  34. Kim YT, Nguyen B-P, Yun D-H (2018) Analysis of consolidation behavior of PVD-improved ground considering a varied discharge capacity. *Eng Comput* 35:1183–1202. <https://doi.org/10.1108/EC-06-2017-0199>
  35. Kim P, Ri K-S, Kim Y-G et al (2020) Nonlinear consolidation analysis of a saturated clay layer with variable compressibility



- and permeability under various cyclic loadings. *Int J Geomech* 20:04020111. [https://doi.org/10.1061/\(asce\)gm.1943-5622.0001730](https://doi.org/10.1061/(asce)gm.1943-5622.0001730)
36. Lei GH, Zheng Q, Ng CWW et al (2015) An analytical solution for consolidation with vertical drains under multi-ramp loading. *Géotechnique* 65:531–541. <https://doi.org/10.1680/geot.13.P.196>
  37. Lekha KR, Krishnaswamy NR, Basak P (1998) Consolidation of clay by sand drain under time-dependent loading. *J Geotech Geoenviron Eng* 124:91–94. [https://doi.org/10.1061/\(ASCE\)1090-0241\(1998\)124:1\(91\)](https://doi.org/10.1061/(ASCE)1090-0241(1998)124:1(91))
  38. Lekha KR, Krishnaswamy NR, Basak P (2003) Consolidation of clays for variable permeability and compressibility. *J Geotech Geoenviron Eng* 129:1001–1009. [https://doi.org/10.1061/\(asce\)1090-0241\(2003\)129:11\(1001\)](https://doi.org/10.1061/(asce)1090-0241(2003)129:11(1001))
  39. Leo CJ (2004) Equal strain consolidation by vertical drains. *J Geotech Geoenviron Eng* 130:316–327. [https://doi.org/10.1061/\(asce\)1090-0241\(2004\)130:3\(316\)](https://doi.org/10.1061/(asce)1090-0241(2004)130:3(316))
  40. Li YC, Cleall PJ (2013) Consolidation of sensitive clays: a numerical investigation. *Acta Geotech* 8:59–66. <https://doi.org/10.1007/s11440-012-0171-x>
  41. Liu S, Geng X, Sun H et al (2019) Nonlinear consolidation of vertical drains with coupled radial-vertical flow considering time and depth dependent vacuum pressure. *Int J Numer Anal Methods Geomech* 43:767–780. <https://doi.org/10.1002/nag.2888>
  42. Liu J-C, Lei G-H, Zheng M-X (2014) General solutions for consolidation of multilayered soil with a vertical drain system. *Geotext Geomembr* 42:267–276. <https://doi.org/10.1016/j.geotextmem.2014.04.001>
  43. Liu Y, Zheng JJ, Zhao X et al (2021) A closed-form solution for axisymmetric electro-osmotic consolidation considering smear effects. *Acta Geotech* <https://doi.org/10.1007/s11440-021-01353-z>
  44. Lo DOK (1991) Soil improvement by vertical drains. Ph.D. Dissertation, University of Illinois at Urbana-Champaign
  45. Lu M, Sloan SW, Indraratna B et al (2016) A new analytical model for consolidation with multiple vertical drains. *Int J Numer Anal Methods Geomech* 40:1623–1640. <https://doi.org/10.1002/nag>
  46. Lu M, Wang S, Sloan SW et al (2015) Nonlinear radial consolidation of vertical drains under a general time-variable loading. *Int J Numer Anal Methods Geomech* 39:51–62. <https://doi.org/10.1002/nag>
  47. Lu M, Wang S, Sloan SW et al (2015) Nonlinear consolidation of vertical drains with coupled radial-vertical flow considering well resistance. *Geotext Geomembr* 43:182–189. <https://doi.org/10.1016/j.geotextmem.2014.12.001>
  48. Lu MM, Xie KH, Wang SY (2011) Consolidation of vertical drain with depth-varying stress induced by multi-stage loading. *Comput Geotech* 38:1096–1101
  49. Nguyen B-P (2021) Nonlinear analytical modeling of vertical drain-installed soft soil considering a varied discharge capacity. *Geotech Geol Eng* 39:119–134. <https://doi.org/10.1007/s10706-020-01477-1>
  50. Nguyen BP, Kim YT (2019) An analytical solution for consolidation of PVD-installed deposit considering nonlinear distribution of hydraulic conductivity and compressibility. *Eng Comput* 36:707–730. <https://doi.org/10.1108/EC-04-2018-0196>
  51. Nogami T, Li M (2003) Consolidation of clay with a system of vertical and horizontal drains. *J Geotech Geoenviron Eng* 129:838–848. [https://doi.org/10.1061/\(ASCE\)1090-0241\(2003\)129:9\(838\)](https://doi.org/10.1061/(ASCE)1090-0241(2003)129:9(838))
  52. Olsen-Kettle (2011) Numerical solution of partial differential equations. Brisbane
  53. Onoue A (1988) Consolidation by vertical drains taking well resistance and smear into consideration. *Soils Found* 28:165–174. [https://doi.org/10.3208/sandf1972.28.4\\_165](https://doi.org/10.3208/sandf1972.28.4_165)
  54. Onoue A (1988) Consolidation of multilayered anisotropic soils by vertical drains with well resistance. *Soils Found* 28:75–90. [https://doi.org/10.3208/sandf1972.28.3\\_75](https://doi.org/10.3208/sandf1972.28.3_75)
  55. Richart FE (1957) A review of the theories for sand drains. *J Soil Mech Found Div* 83:1301–1338. <https://doi.org/10.1061/JSEFAQ.0000064>
  56. Rujikiatkamjorn C, Indraratna B (2007) Analytical solutions and design curves for vacuum-assisted consolidation with both vertical and horizontal drainage. *Can Geotech J* 44:188–200. <https://doi.org/10.1139/T06-111>
  57. Rujikiatkamjorn C, Indraratna B (2010) Radial consolidation modelling incorporating the effect of a smear zone for a multi-layer soil with downdrag caused by mandrel action. *Can Geotech J* 47:1024–1035. <https://doi.org/10.1139/T09-149>
  58. Sathananthan I, Indraratna B (2006) Plane-strain lateral consolidation with non-Darcian flow. *Can Geotech J* 43:119–133. <https://doi.org/10.1139/t05-094>
  59. Seah TH, Juirnarongrit T (2003) Constant rate of strain consolidation with radial drainage. *Geotech Test J* 26:432–443. <https://doi.org/10.1520/gtj11251j>
  60. Shen SL, Chai JC, Hong ZS, Cai FX (2005) Analysis of field performance of embankments on soft clay deposit with and without PVD-improvement. *Geotext Geomembr* 23:463–485. <https://doi.org/10.1016/j.geotextmem.2005.05.002>
  61. Tang X, Niu B, Cheng G, Shen H (2013) Closed-form solution for consolidation of three-layer soil with a vertical drain system. *Geotext Geomembr* 36:81–91. <https://doi.org/10.1016/j.geotextmem.2012.12.002>
  62. Tang X-W, Onitsuka K (2000) Consolidation by vertical drains under time-dependent loading. *Int J Numer Anal Methods Geomech* 24:739–751. [https://doi.org/10.1002/1096-9853\(20000810\)24:93.0.CO;2-B](https://doi.org/10.1002/1096-9853(20000810)24:93.0.CO;2-B)
  63. Tang X-W, Onitsuka K (2001) Consolidation of double-layered ground with vertical drains. *Int J Numer Anal Methods Geomech* 25:1449–1465. <https://doi.org/10.1002/nag.191>
  64. Tavenas F, Jean P, Leblond P, Leroueil S (1983) The permeability of natural soft clays. Part II: permeability characteristics. *Can Geotech J* 20:645–659. <https://doi.org/10.1139/t83-072>
  65. Tian Y, Wu W, Jiang G et al (2019) Analytical solutions for vacuum preloading consolidation with prefabricated vertical drain based on elliptical cylinder model. *Comput Geotech* 116:103202. <https://doi.org/10.1016/j.compgeo.2019.103202>
  66. Tian Y, Wu W, Wen M et al (2021) Nonlinear consolidation of soft foundation improved by prefabricated vertical drains based on elliptical cylindrical equivalent model. *Int J Numer Anal Methods Geomech* 45:1949–1971. <https://doi.org/10.1002/nag.3250>
  67. Trefethen LN (2000) Spectral methods in MATLAB. Society for Industrial and Applied Mathematics, Philadelphia
  68. Walker RT (2011) Vertical drain consolidation analysis in one, two and three dimensions. *Comput Geotech* 38:1069–1077. <https://doi.org/10.1016/j.compgeo.2011.07.006>
  69. Walker R, Indraratna B (2006) Vertical drain consolidation with parabolic distribution of permeability in smear zone. *J Geotech Geoenvironmental Eng* 132:937–941. [https://doi.org/10.1061/\(ASCE\)1090-0241\(2006\)132:7\(937\)](https://doi.org/10.1061/(ASCE)1090-0241(2006)132:7(937))
  70. Walker R, Indraratna B (2007) Vertical drain consolidation with overlapping smear zones. *Géotechnique* 57:463–467. <https://doi.org/10.1680/geot.2007.57.5.463>
  71. Walker R, Indraratna B (2009) Consolidation analysis of a stratified soil with vertical and horizontal drainage using the spectral method. *Géotechnique* 59:439–449. <https://doi.org/10.1680/geot.2007.00019>
  72. Walker RTR, Indraratna B (2015) Application of spectral Galerkin method for multilayer consolidation of soft soils



- stabilised by vertical drains or stone columns. *Comput Geotech* 69:529–539. <https://doi.org/10.1016/j.compgeo.2015.06.015>
73. Walker R, Indraratna B, Rujikiatkamjorn C (2012) Vertical drain consolidation with non-Darcian flow and void-ratio dependent compressibility and permeability. *Géotechnique* 62:985–997. <https://doi.org/10.1680/geot.10.P.084>
74. Walker R, Indraratna B, Sivakugan N (2009) Vertical and radial consolidation analysis of multilayered soil using the spectral method. *J Geotech Geoenviron Eng* 135:657–663. [https://doi.org/10.1061/\(ASCE\)GT.1943-5606.0000075](https://doi.org/10.1061/(ASCE)GT.1943-5606.0000075)
75. Wang L, Huang P, Liu S, Alonso E (2020) Analytical solution for nonlinear consolidation of combined electroosmosis-vacuum-surchage preloading. *Comput Geotech* 121:103484. <https://doi.org/10.1016/j.compgeo.2020.103484>
76. Xie KH (1987) Sand drained ground: analytical and numerical solutions and optimal design. Ph.D. Dissertation, Zhejiang University
77. Xu B-H, He N, Jiang Y-B et al (2020) Experimental study on the clogging effect of dredged fill surrounding the PVD under vacuum preloading. *Geotext Geomembr* 48:614–624. <https://doi.org/10.1016/j.geotextmem.2020.03.007>
78. Xu B-H, Indraratna B, Nguyen TT, Walker R (2021) A vertical and radial consolidation analysis incorporating drain degradation based on the spectral method. *Comput Geotech* 129:103862. <https://doi.org/10.1016/j.compgeo.2020.103862>
79. Xu B-H, He N, Zhou Y-Z et al (2021) Nonlinear consolidation model for stratified soils with vertical drains based on spectral method. *Chinese J Geotech Eng* 43(10):1781–1788. (in Chinese)
80. Xu B-H, Indraratna B, Rujikiatkamjorn C, Nguyen T T (2022) A large-strain radial consolidation model incorporating soil destructuration and isotache concept. *Comput Geotech* 147:104761. <https://doi.org/10.1016/j.compgeo.2022.104761>
81. Yoshikuni H, Nakanodo H (1974) Consolidation of soils by vertical drain wells with finite permeability. *Soils Found* 14:35–46. [https://doi.org/10.3208/sandf1972.14.2\\_35](https://doi.org/10.3208/sandf1972.14.2_35)
82. Zeng GX, Xie KH (1989) New development of the vertical drain theories. In: Proceedings of the 12th international conference on soil mechanics and foundation engineering. Rio de Janeiro, Brazil, pp 1435–1438
83. Zhou WH, Lok TMH, Zhao LS et al (2017) Analytical solutions to the axisymmetric consolidation of a multi-layer soil system under surcharge combined with vacuum preloading. *Geotext Geomembr* 45:487–498. <https://doi.org/10.1016/j.geotextmem.2017.06.003>
84. Zhou Y, Wang P, Shi L et al (2021) Analytical solution on vacuum consolidation of dredged slurry considering clogging effects. *Geotext Geomembr* 49:842–851. <https://doi.org/10.1016/j.geotextmem.2020.12.013>
85. Zhu GF, Yin JH (2004) Consolidation analysis of soil with vertical and horizontal drainage under ramp loading considering smear effects. *Geotext Geomembr* 22:63–74. [https://doi.org/10.1016/S0266-1144\(03\)00052-9](https://doi.org/10.1016/S0266-1144(03)00052-9)

**Publisher's Note** Springer Nature remains neutral with regard to jurisdictional claims in published maps and institutional affiliations.